Fragility functions for regional assessment of infilled RC buildings: analytical derivation and empirical validation

Speaker: **Al Mouayed Bellah Nafeh** – IUSS Pavia

When: **7h November 2023 17:00 CET**

Where: **Sala del Camino, Piazza della Vittoria 15, Pavia**

https://iusspavia.zoom.us/j/84927730399



IUSS
Scuola Universitaria Superiore Pavia

ROSE Centre
Centre for Training and Research on Reduction of Seismic Risk

Web: www.iusspavia.it/rose Email: rose@iusspavia.it

Outline

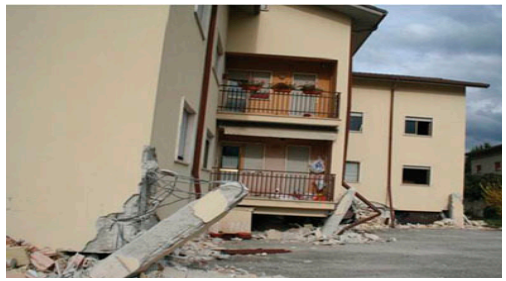
- Motivation
- Derivation of analytical fragility functions
- Derivation of empirical fragility functions
- Verification & Discussion
- Conclusions

Motivation

- Complex structural system
- Additional complexity for existing structures designed prior to the introduction of modern seismic guidelines
- Brittle non-ductile failure mechanisms (e.g., shear failures expected to occur in columns)
- Past earthquakes highlighted their increased vulnerability to ground-shaking



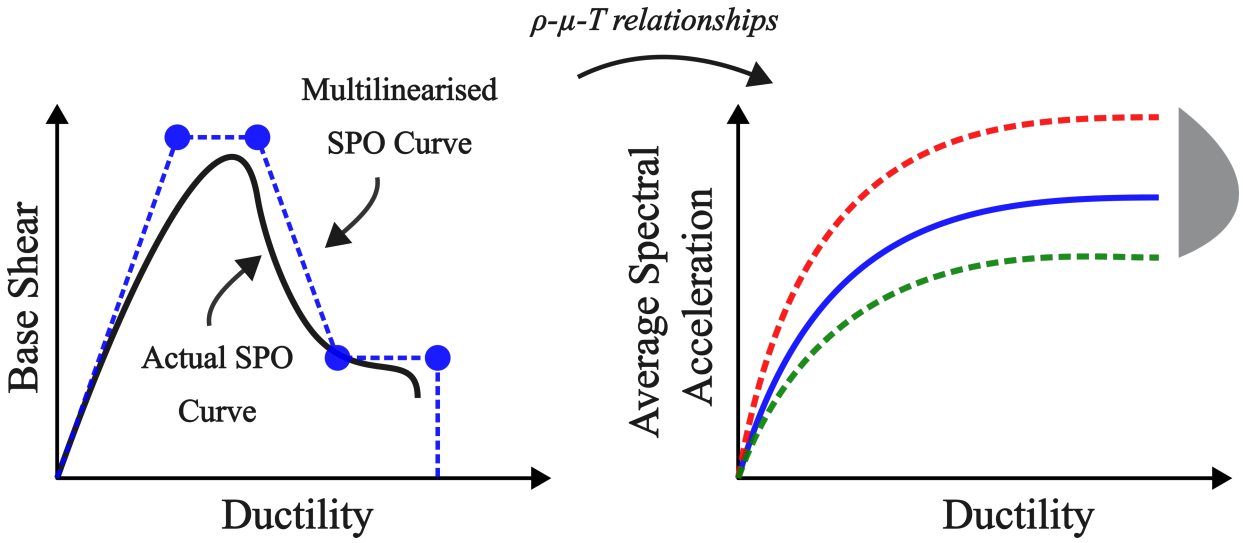


Motivation

Q: How to eliminate bias in the structural response due to the excessive scaling of ground-motion records in incremental dynamic analysis?

A: cloud-based $\rho - \mu - T$ relationships for the direct capacity-to-demand estimation using Saavg as the IM

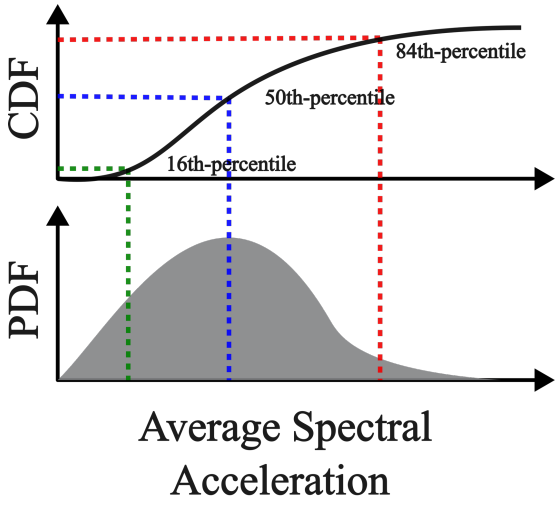


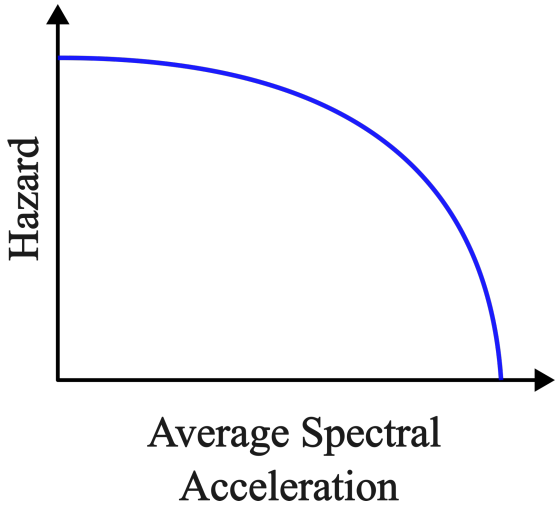
Al Mouayed Bellah Nafeh, Gerard J. O'Reilly, Unbiased simplified seismic fragility estimation of non-ductile infilled RC structures, Soil Dynamics and Earthquake Engineering, Volume 157, 2022,107253, ISSN 0267-7261, https://doi.org/10.1016/j.soildyn.2022.107253.

Motivation

Q: Do current risk classification schemes communicate uniform risk estimates? What is the metric to be adopted for risk classification schemes of existing structures?

A: PB-Risk: pushover-based seismic risk assessment framework for the calculation of the MAFE or λ



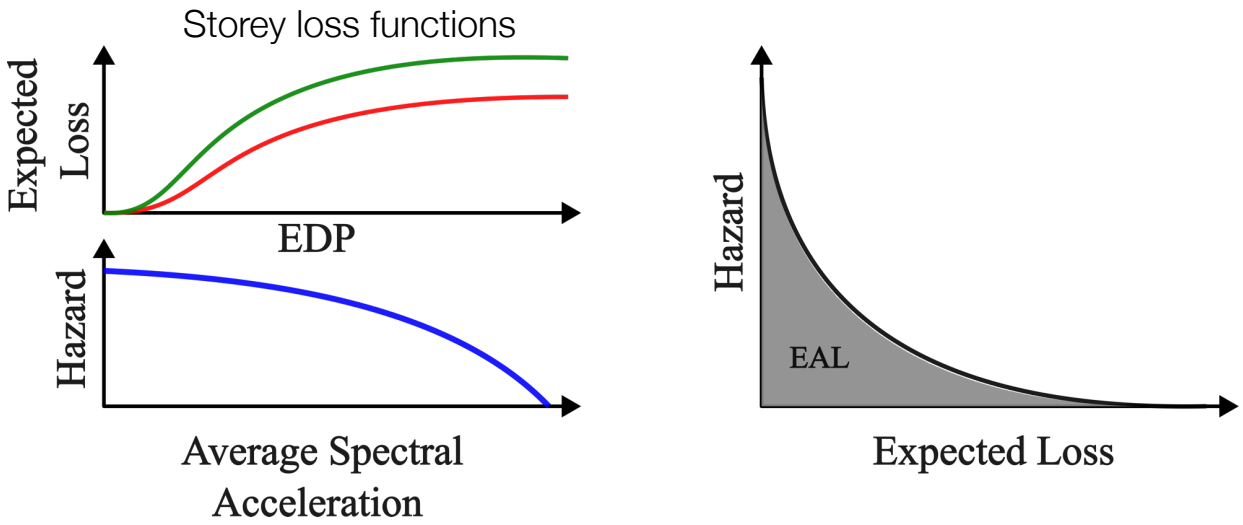


Nafeh, A.M.B., O'Reilly, G.J. Simplified pushover-based seismic risk assessment methodology for existing infilled frame structures. *Bull Earthquake Eng* **21**, 2337–2368 (2023). https://doi.org/10.1007/s10518-022-01600-y

Motivation

Q: Can we estimate robustly and more efficiently the direct economic losses due to earthquake events?

A: PB-Loss: pushover-based seismic loss assessment framework using generalized storey-loss functions



Nafeh, A.M.B., O'Reilly, G.J. Simplified pushover-based seismic loss assessment for existing infilled frame structures. *Bull Earthquake Eng* (2023). https://doi.org/10.1007/s10518-023-01792-x

Motivation

Q: What is the common factor among the simplified methodologies presented in previous work?

A: The average spectral acceleration ($Sa_{avg}(T^*)$) is the intensity measure

- The average spectral acceleration was first introduced in the early 2000s as an efficient IM for response prediction

$$Sa_{avg}(T^*) = \left(\prod_{i=1}^{N} Sa(c_i T^*)\right)^{\frac{1}{N}}$$

- c_i represents N=10 number coefficients in the range of 0.2-3.0 and T^* is the anchoring period;
- The select array of periods covers higher mode response and “period elongation” due to the reduction in initial stiffness due to damage accumulation
- High efficiency, sufficiency, practicality

Q: Can we derive reliable analytical fragility functions for the regional assessment of infilled RC frame buildings?



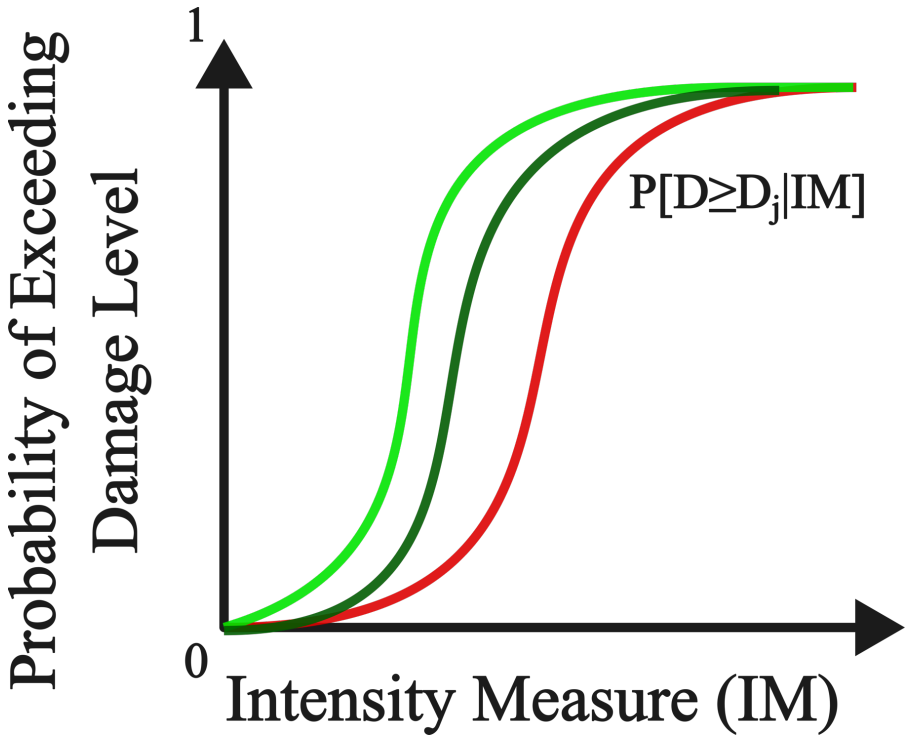
Analytical Fragility Functions

Derivation of state-of-the-art typological fragility functions using average spectral acceleration

General Notions

- Fragility curves or functions (FFs) quantify the exceedance probability of any structural demand-based performance level, or limit state as a function of the ground shaking intensity

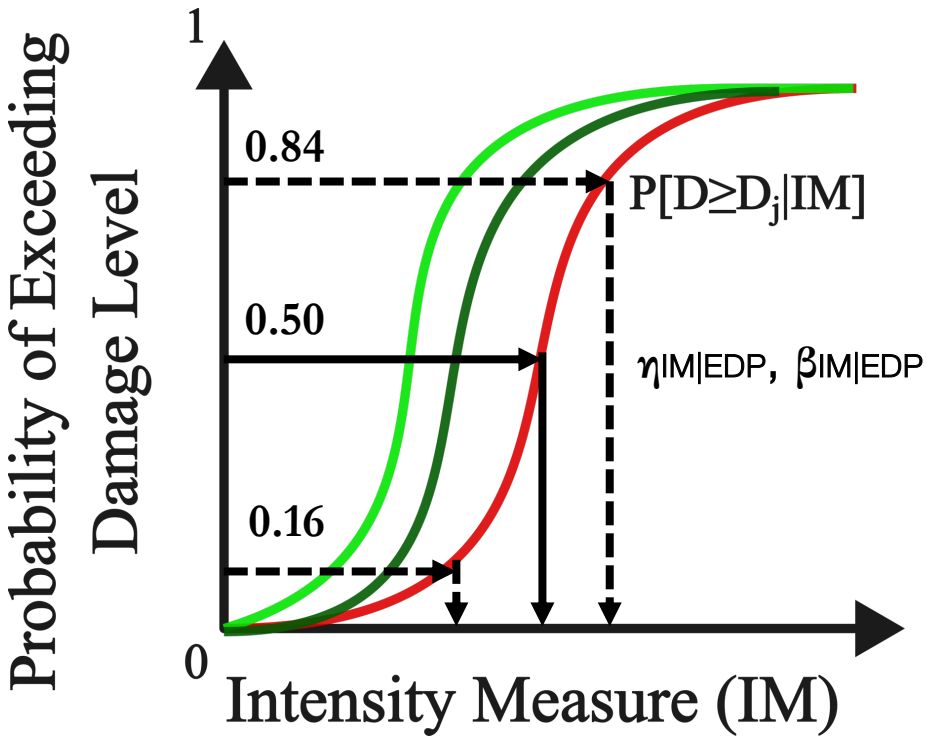
- FFs can be derived analytically, empirically, heuristically or via a hybrid approach



General Notions

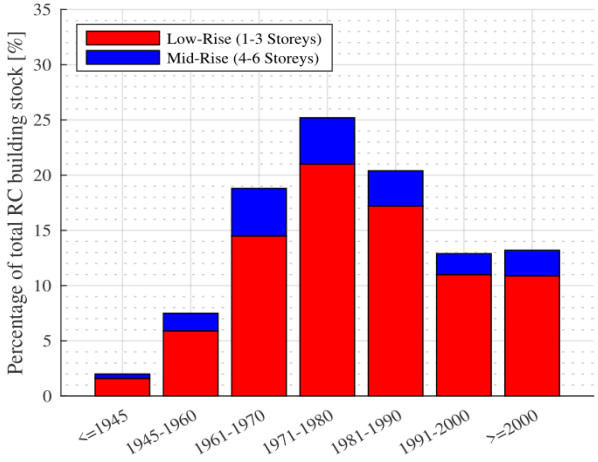
- FFs are typically represented via a lognormal CDF
- The median intensity, $\eta_{IM|EDP}$ for a given damage level is the *IM* corresponding to 50% probability of exceedance on the FF
- The logarithmic standard deviation or dispersion of the equivalent lognormal FF, $\beta_{IM|EDP}$, is estimated as

$$\beta_{IM|EDP} = \frac{\ln(IM_{84\%} - IM_{16\%})}{2}$$

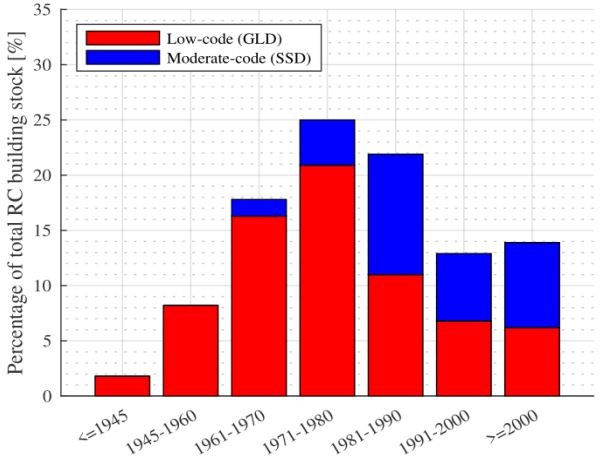


Building Class Definition

- The definition of a building class is a key step towards assessing seismic risk.
- Building classes must be defined using building attributes relevant to seismic vulnerability, such as load-bearing system, lateral load-resisting system, height or date of construction
- Taxonomies must also be simple to remain familiar and applicable to other users, but also comprehensive to maintain relevance in how they describe the seismic performance of different construction types.



Number of Stories



Design Code Level

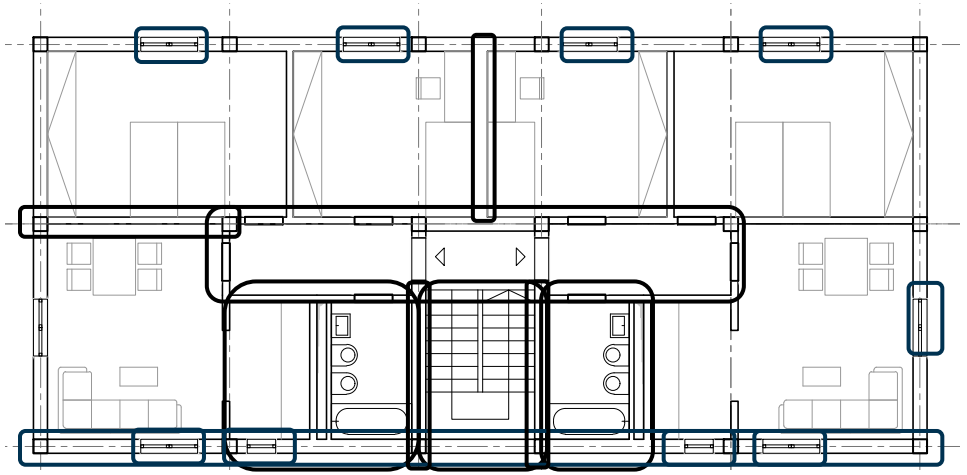
Building Class Definition

- The definition of a building class is a key step towards assessing seismic risk.
- Building classes must be defined using building attributes relevant to seismic vulnerability, such as load-bearing system, lateral load-resisting system, height or date of construction
- Taxonomies must also be simple to remain familiar and applicable to other users, but also comprehensive to maintain relevance in how they describe the seismic performance of different construction types.

Building Class	Sub-Taxonomy Code	Description
Low-code low-rise infilled RC buildings	LC-LR	• LC (low-code): refers to structures designed for gravity loads only and no consideration to ductile detailing; • MC (moderate-code): refers to structures designed according to the ELF method with a seismic coefficient of 7% and no consideration to ductile detailing; • LR (low-rise): refers to structures with 1-3 storeys above ground; • MR (mid-rise): refers to structures with 4-6 storeys above ground;
Low-code mid-rise infilled RC buildings	LC-MR	
Moderate-code low-rise infilled RC buildings	MC-LR	
Moderate-code mid-rise infilled RC buildings	MC-MR	

Archetype Design: Architecture

- FFs for a class can be derived by assuming the portfolio of buildings in a class is replaced by an “average” representative building
- Expert architectural judgement (i.e. consultation with practitioners and review of past guidelines)
- Representative geometric configuration and architectural features, for example:
  - Narrow hallways and corridors in dwellings, generally 150 cm wide
  - Staircase width not exceeding 3 m (i.e. wide enough to allow the passage of two people) and landings depth not exceeding 1.3 m
  - 30 cm infill panels for the separation of dwellings and encasing of the staircase
  - 80 mm single-leaf masonry infills for Internal partitioning of the living space



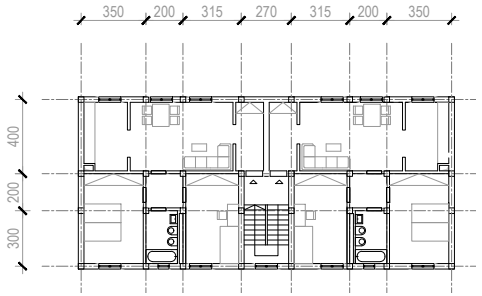
Typical residential RC building layout and key architectural features

Archetype Design: Structural Configuration

Definition of the design and detailing consideration for the conception of archetype numerical building models

Archetype Design Consideration	Construction Era	Design Methodology	Design Considerations
Gravity-Load Design (GLD)	Pre-1970s	Gravity Loads + Allowable Stress Method (Royal Decree 2229/39)	• Frames spanning in one direction • Smooth rebars with low yield strength (Aq42, ($\sigma_{all,s} \approx$ 140 MPa) • Concrete with low compressive strength ($\sigma_{all,c} \approx$ 5 MPa) • Poor transverse detailing and low shear reinforcement ratios • Inadequate detailing of beam-column joints
Sub-Standard Design (SSD)	1970s-1980s	Equivalent Lateral Force Method + Allowable Stress Method (L. 1086/71, DM 40/1975, DM 108/1986)	• Frames spanning in one (or both) directions • Deformed rebars with moderate yield strengths (FeB44k, $\sigma_{all,s} \approx$ 260 MPa) • Concrete with moderate compressive strength ($\sigma_{all,c} \approx$ 7.5 MPa) • No consideration for ductile detailing

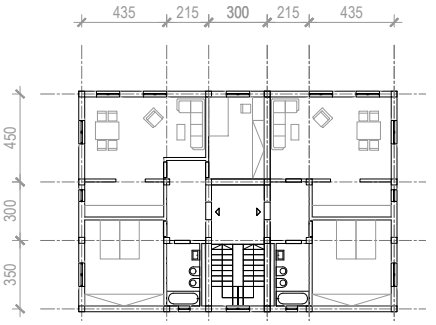
Archetype Design: Database



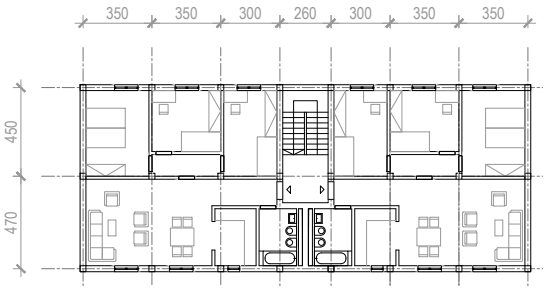
Archetype A



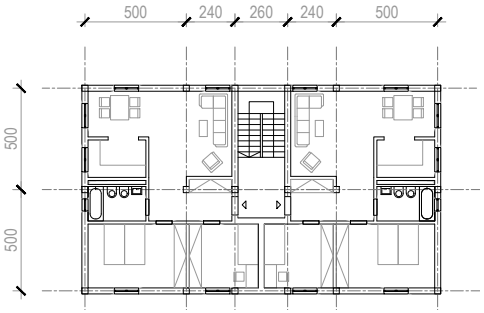
Archetype B



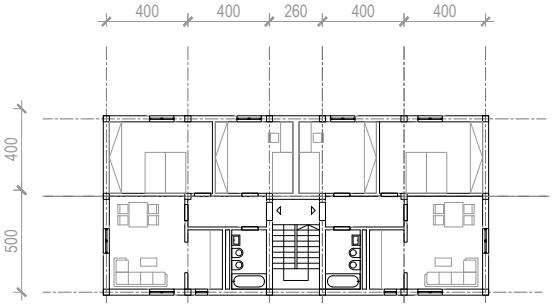
Archetype C



Archetype D



Archetype E

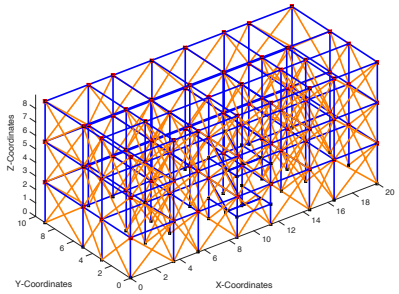


Archetype F

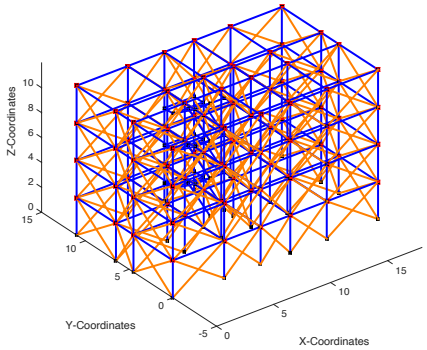


Archetype G

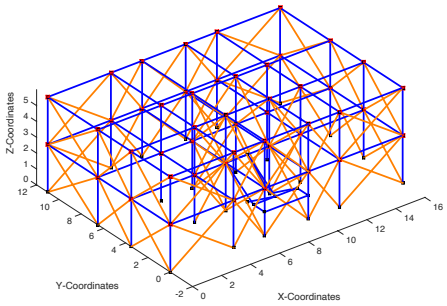
Archetype Design: Database



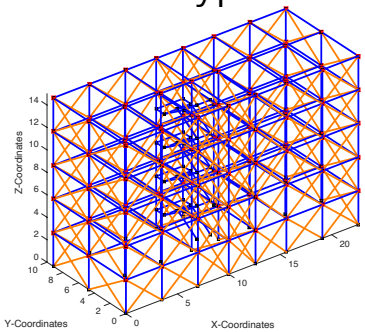
Archetype A



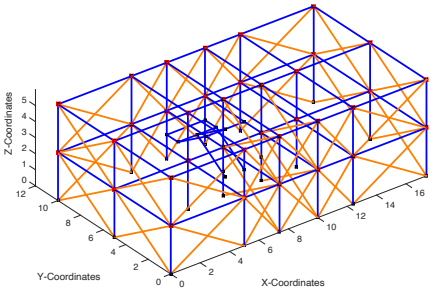
Archetype B



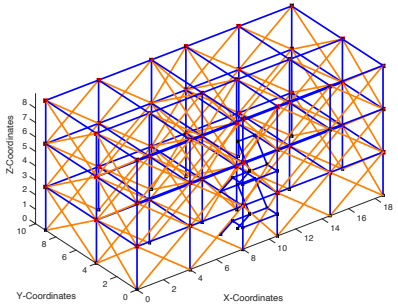
Archetype C



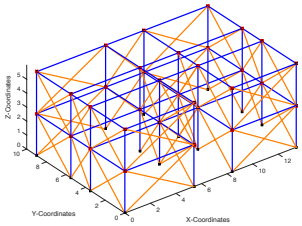
Archetype D



Archetype E



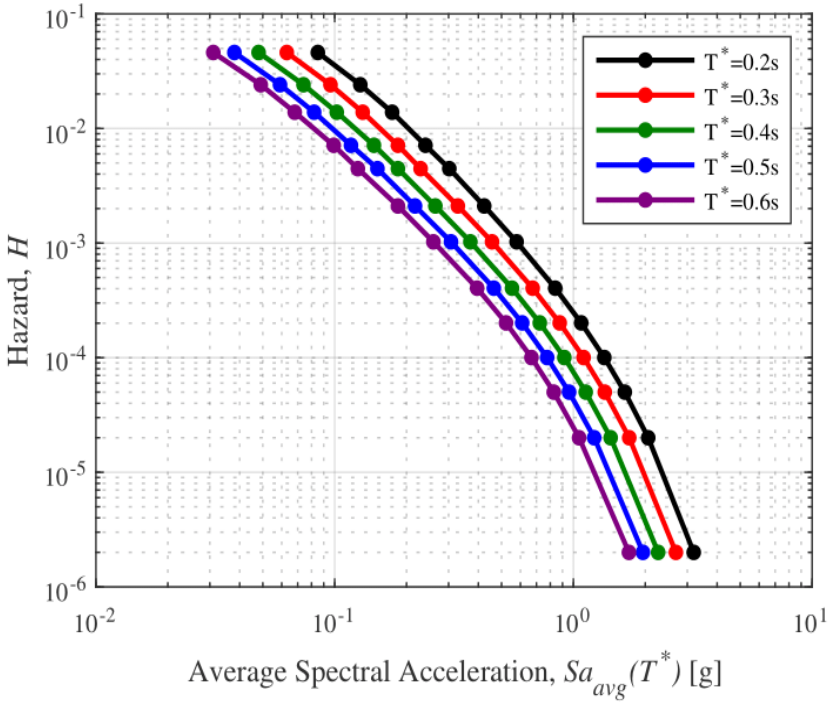
Archetype F



Archetype G

Probabilistic Seismic Hazard Assessment

- OpenQuake Engine
- Location: L'Aquila, Italy
- IM: $Sa_{avg}(T^*)$ where T^* = 0.2 – 0.6 s
- Seismic hazard model: ESHM20
- Site Characterisation: Mori *et al.* (2020)



Average spectral acceleration hazard curves for distinct periods of vibration

Damage States Definition

- Damage states related observed structural damage to consequences like building functionality, economic losses and casualties
- Practice-based applications typically refer to damage states as limit states
- Limit states are triggered by several potential local and global factors (i.e., global displacement-based, local-deformation-based, local strength-based criteria)

Limit-State	Description	NTC18 Thresholds
Stato Limite di Operatività 'Operational' (SLO)	Structural and non-structural elements maintain functionality without suffering damage and significant interruption of usage.	$\theta_{max} = 0.33$ %
Stato Limite di Danno 'Damage Control' (SLD)	Structural and non-structural elements suffer moderate damage.	min $\{\theta_{y,beam}; \theta_{y,column}\}$
Stato Limite di salvaguardia della Vita 'Life Safety' (SLV)	Structure sustains heavy damage to its structural elements resulting in a significant loss of lateral stiffness.	min $\{0.75\theta_{ult,beam}; 0.75\theta_{ult,column}; V_{y,beam}; V_{y,column}, M_{y,\ joint}\}$;
Stato Limite di prevenzione del Collasso 'Collapse Prevention' (SLC)	Structural and non-structural elements suffer heavy damage.	min $\{0.80\ V_{max}; \gamma_{ult,joint}; \theta_{ult,beam}; \theta_{ult,column}\}$
Collapse	Complete collapse of the structure	-

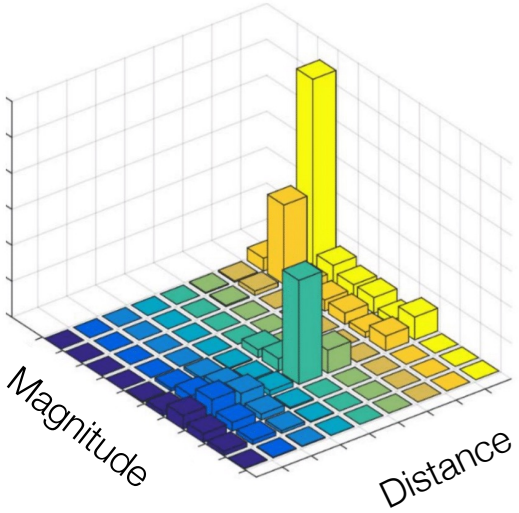
Damage States Definition

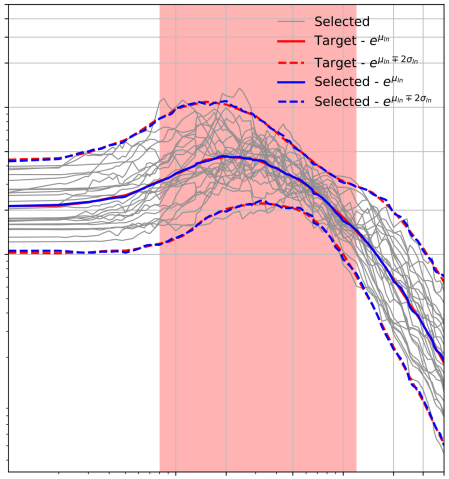
- In non-ductile infilled RC frames, DSs are impacted by the premature failure of the infill panels
- Recent experimental tests (Kurukalasuriya *et al.*) demonstrated that for serviceability, DSs are governed by the in-plane drifts sustained by the infill panels
- Hybrid definition of DSs thresholds was adopted and a collapse DS was added

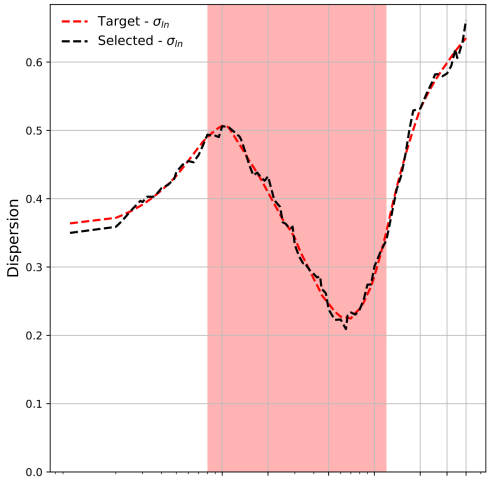
Limit-State	Description	Hybrid Thresholds
Stato Limite di Operatività 'Operational' (SLO)	Structural and non-structural elements maintain functionality without suffering damage and significant interruption of usage.	θ_{max} = 0.16 %
Stato Limite di Danno 'Damage Control' (SLD)	Structural and non-structural elements suffer moderate damage.	θ_{max} = 0.29 %
Stato Limite di salvaguardia della Vita 'Life Safety' (SLV)	Structure sustains heavy damage to its structural elements resulting in a significant loss of lateral stiffness.	min {0.75 $\Delta_{roof,SLC}$; 0.75 $\theta_{ult,beam}$; 0.75$\theta_{ult,column}$; }
Stato Limite di prevenzione del Collasso 'Collapse Prevention' (SLC)	Structural and non-structural elements suffer heavy damage.	min {0.80 V_{max}; $\theta_{ult,beam}$; $\theta_{ult,column}$}
Collapse	Complete collapse of the structure	θ_{max} = 5.0 %

Seismic Performance Assessment

- NTLHA method: Multiple-stripe analyses
- Hazard-consistent ground-motion records selected using EzGM toolbox
- Nine intensity measure levels corresponding to return periods of 22-4975 years
- Scaling factor threshold of 2.0
- Structural response was characterised in terms of the maximum peak storey drift (θ_{max})
- A drawback of MSA for this application is that each archetype building model was evaluated using a slightly different definition of $Sa_{avg}(T^*)$

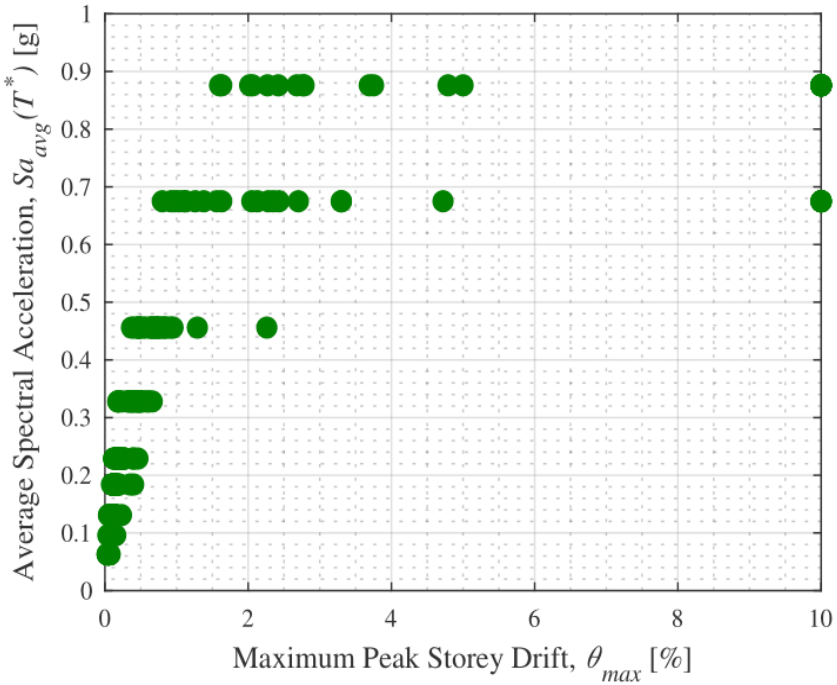






Seismic Performance Assessment

- NTLHA method: Multiple-stripe analyses
- Hazard-consistent ground-motion records selected using EzGM toolbox
- Nine intensity measure levels corresponding to return periods of 22-4975 years
- Scaling factor threshold of 2.0
- Structural response was characterised in terms of the maximum peak storey drift (θ_{max})
- A drawback of MSA for this application is that each archetype building model was evaluated using a slightly different definition of $Sa_{avg}(T^*)$



Multiple-stripe analysis results of a case study building

Seismic Performance Assessment

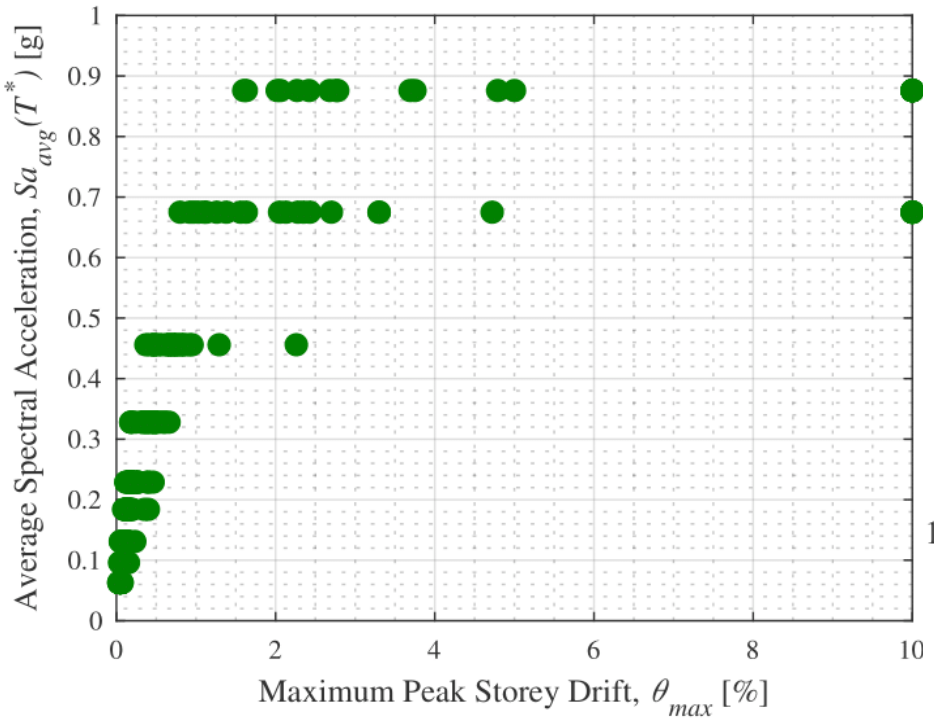
- To characterize buildings under the same taxonomies, buildings were aggregated using single definition for the conditioning period

Sub-Taxonomy Code	Individual Buildings	Grouped Buildings
	Conditioning Period, T^*	Conditioning Period, T^*_{tax}
LC-LR	0.2s and 0.3s for two- and three-storey buildings, respectively	$0.25s$
LC-MR	0.4s, 0.5s and 0.6s for four-, five- and six-storey buildings, respectively	$0.50s$
MC-LR	0.2s and 0.3s for two- and three-storey buildings, respectively	$0.25s$
MC-MR	0.4s, 0.5s and 0.6s for four-, five- and six-storey buildings, respectively	$0.50s$

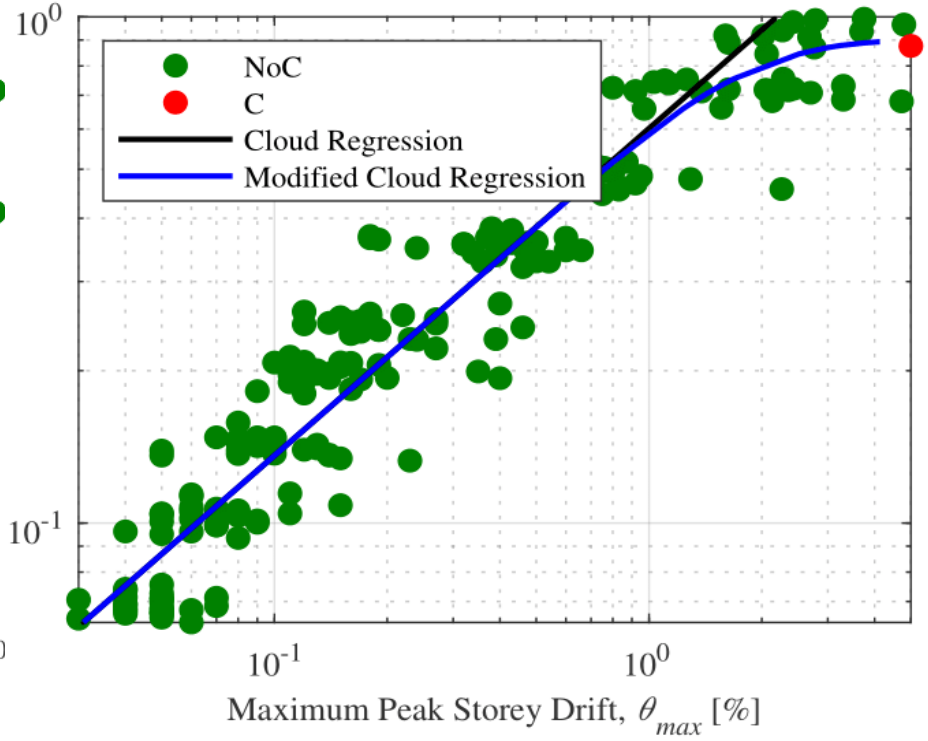
Seismic Performance Assessment

- Due to building grouping, MSA results transform into a “banded cloud” of results
- Results remain hazard-consistent
- A more direct approach is to directly select ground-motion records for MSA in terms of $Sa_{avg}(T^*_{tax})$

MSA

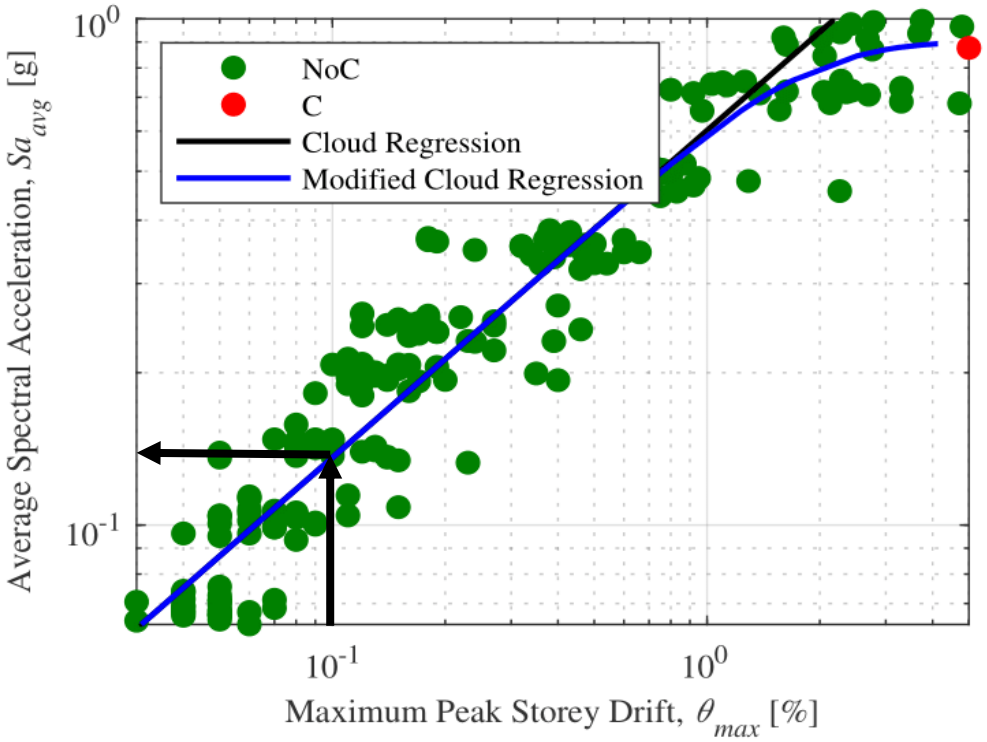


Cloud Analysis



Median Intensity Characterisation: Single Case

$\eta_{IM|\theta_{max}=0.1\%} \approx 0.195g$

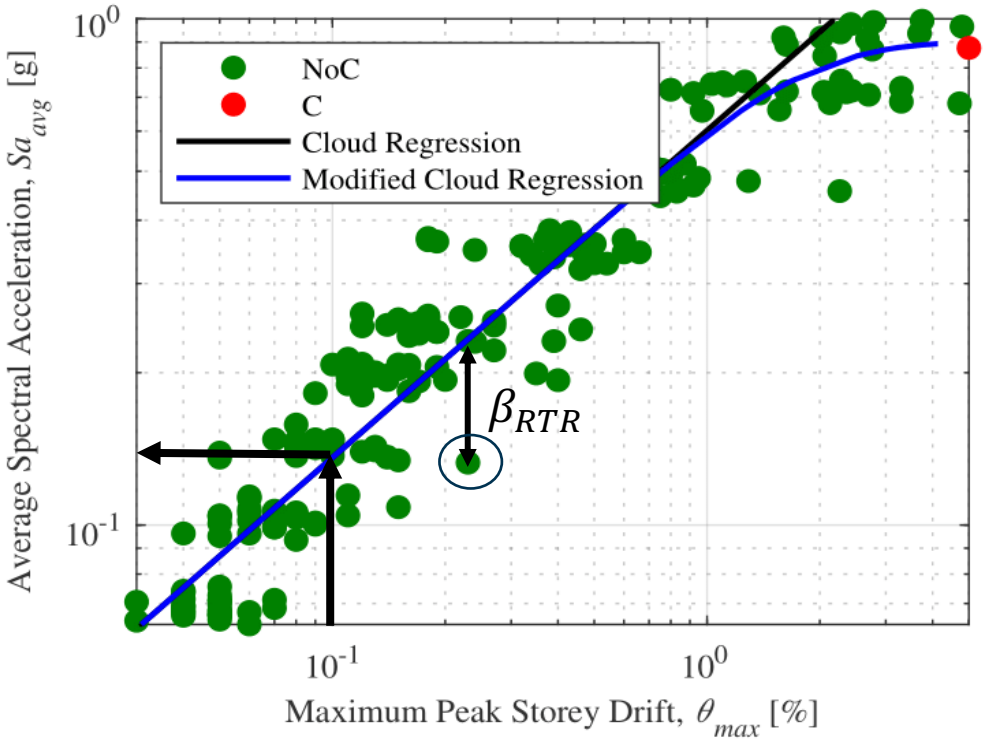


$$log\eta_{IM|EDP} = loga + b\ logEDP$$

Median intensity

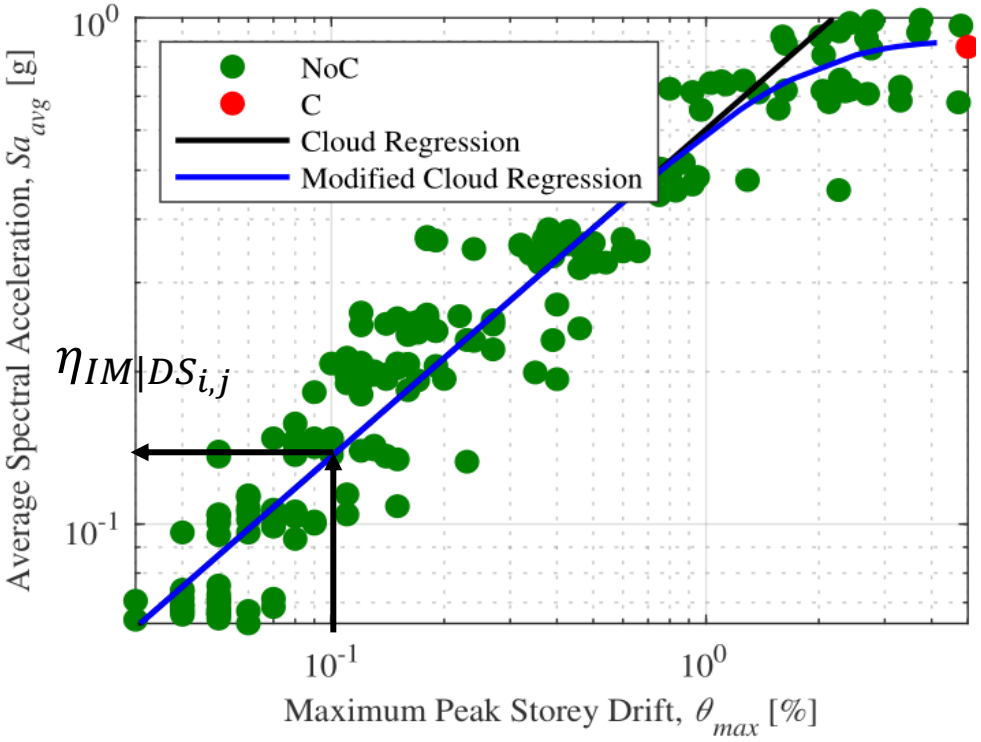
Engineering demand parameter

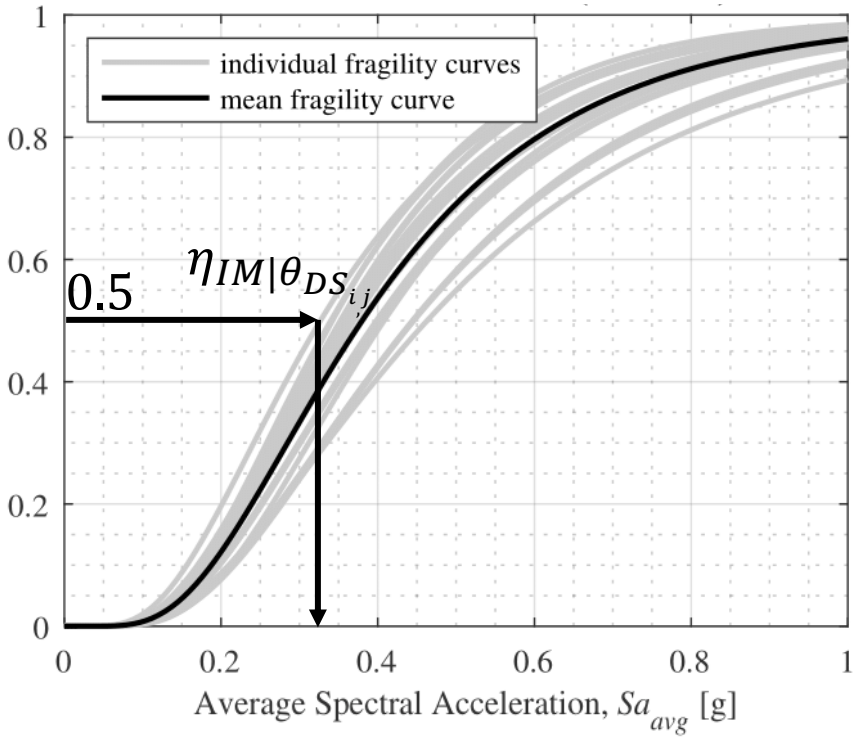
Epistemic Uncertainty: Single Case



$$\beta_{RTR} = \sigma_{logIM|EDP} = \sqrt{\frac{\sum_{i=1}^{n}(logY_i - log\eta_{IM|EDP})^2}{n-2}}$$

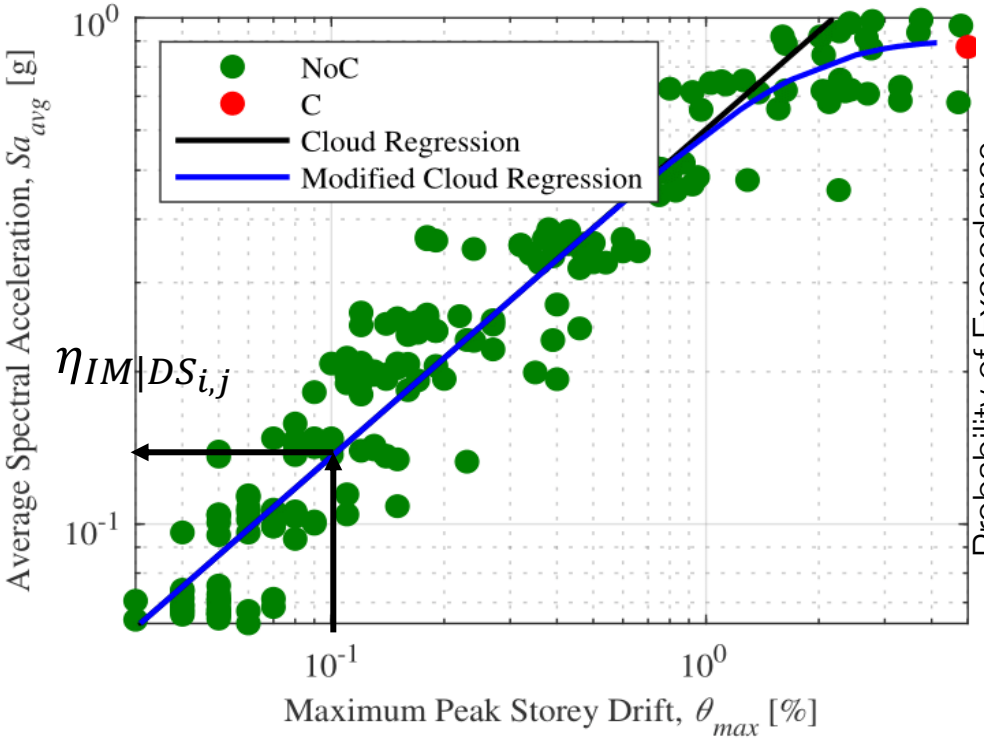
Median Intensity Characterisation: Assets

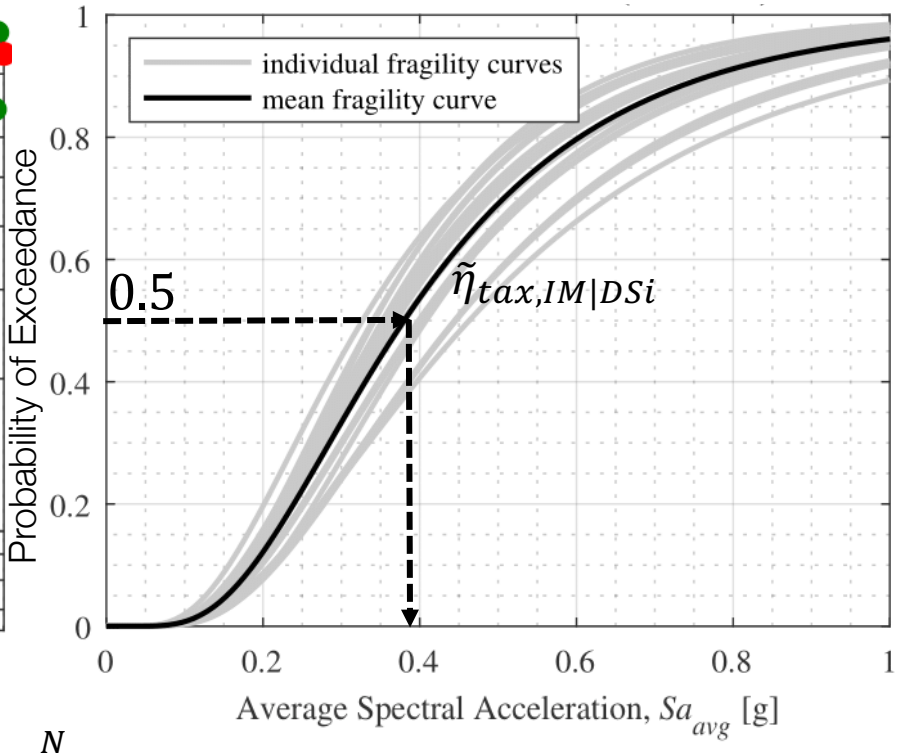




$$\underbrace{log\eta_{IM|DS_{i,j}}}_{\text{Median intensity for building j given DSi}} = loga + b\ \underbrace{logEDP_{DSi,j}}_{\text{Engineering demand parameter for the single-building j given DSi}}$$

Median Intensity Characterisation: Assets





$$\underbrace{\tilde{\eta}_{tax,IM|DSi}}_{\text{Taxonomy mean intensity}} = \frac{1}{N}\sum_{i}^{N} \underbrace{\eta_{IM|DSi}}_{\text{Single-building Median intensity given DS}}$$

Treatment of Uncertainty: Assets

- The performance assessment of any structural typology requires due consideration of both aleatory and epistemic sources of uncertainty
- The aleatory uncertainty is associated with the randomness in ground motion records
- The epistemic uncertainty relates to uncertainties in the numerical modelling
- The law of total variance is used to estimate the total uncertainty associated with a taxonomy class

total dispersion associated with the taxonomy

$$\beta_{lnY_{tax,total}} = \sqrt{\beta^2_{lnY_{intra}} + \beta^2_{lnY_{inter}} + \beta^2_{MDL}}$$

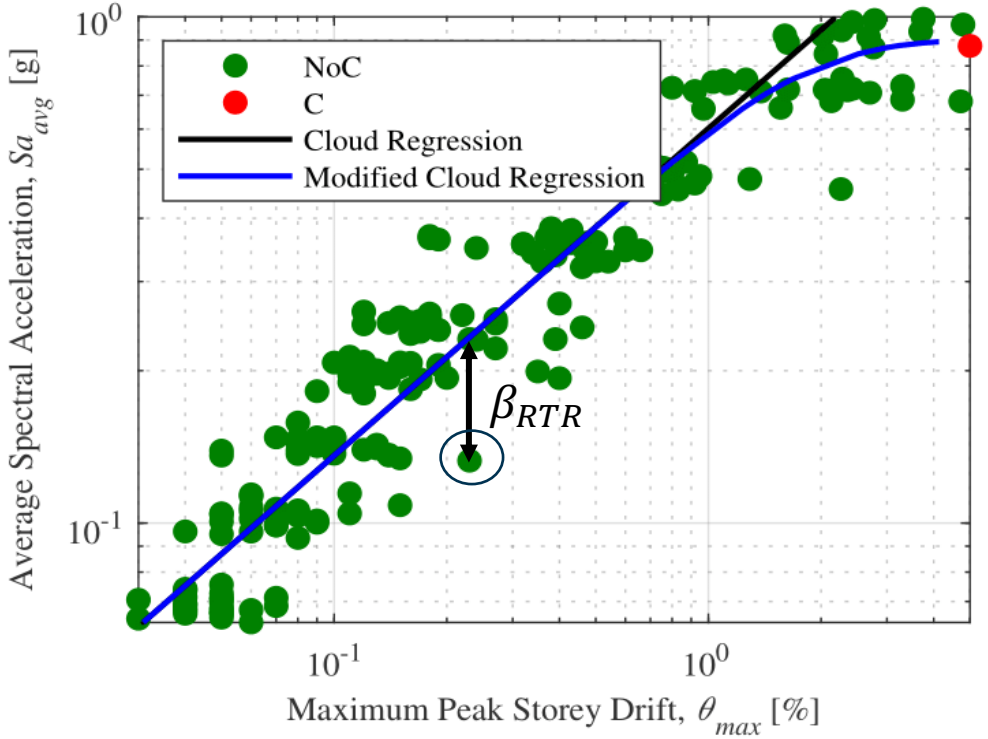
Intra-building variability

Inter-building variability

Modelling uncertainty

Treatment of Uncertainty: Assets

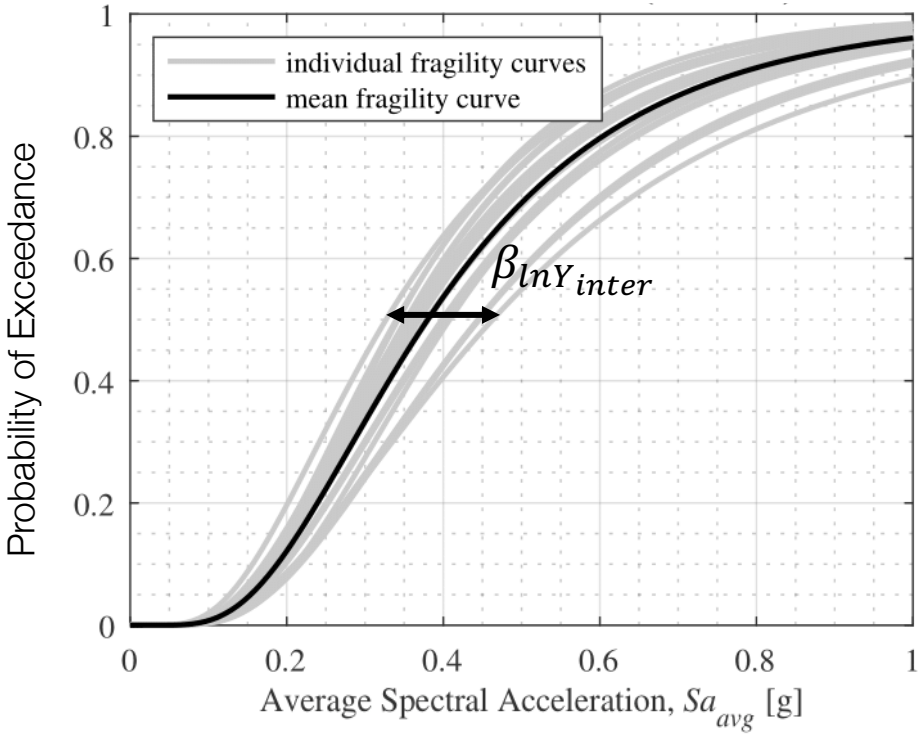
$$\beta_{lnY_{tax,total}} = \sqrt{\beta^2_{lnY_{intra}} + \beta^2_{lnY_{inter}} + \beta^2_{MDL}}$$



$$\beta^2_{lnY_{intra}} = \frac{1}{N}\sum_{i=1}^{N} \beta^2_{RTR,i}$$

Treatment of Uncertainty: Assets

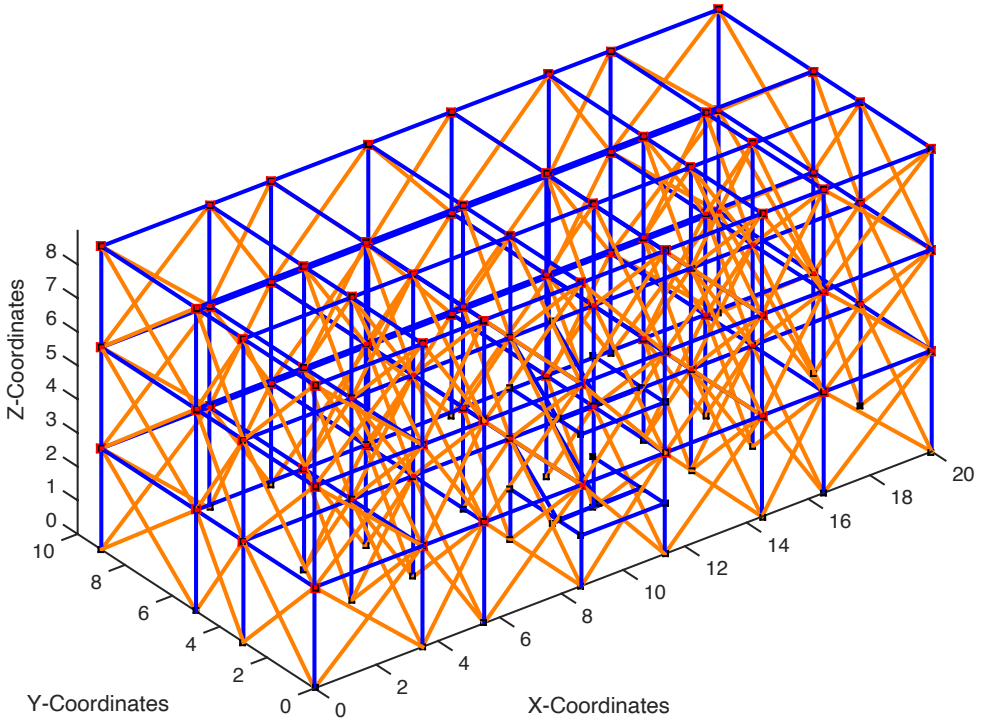
$$\beta_{lnY_{tax,total}} = \sqrt{\beta^2_{lnY_{intra}} + \boxed{\beta^2_{lnY_{inter}}} + \beta^2_{MDL}}$$



$$\beta_{lnY_{inter}} = \sqrt{\frac{\sum_{i=1}^{N}(log\eta_{IM|DSi,j} - log\tilde{\eta}_{IM|DSi})^2}{N}}$$

Treatment of Uncertainty: Assets

$$\beta_{lnY_{tax,total}} = \sqrt{\beta_{lnY_{intra}}^2 + \beta_{lnY_{inter}}^2 + \boxed{\beta_{MDL}^2}}$$



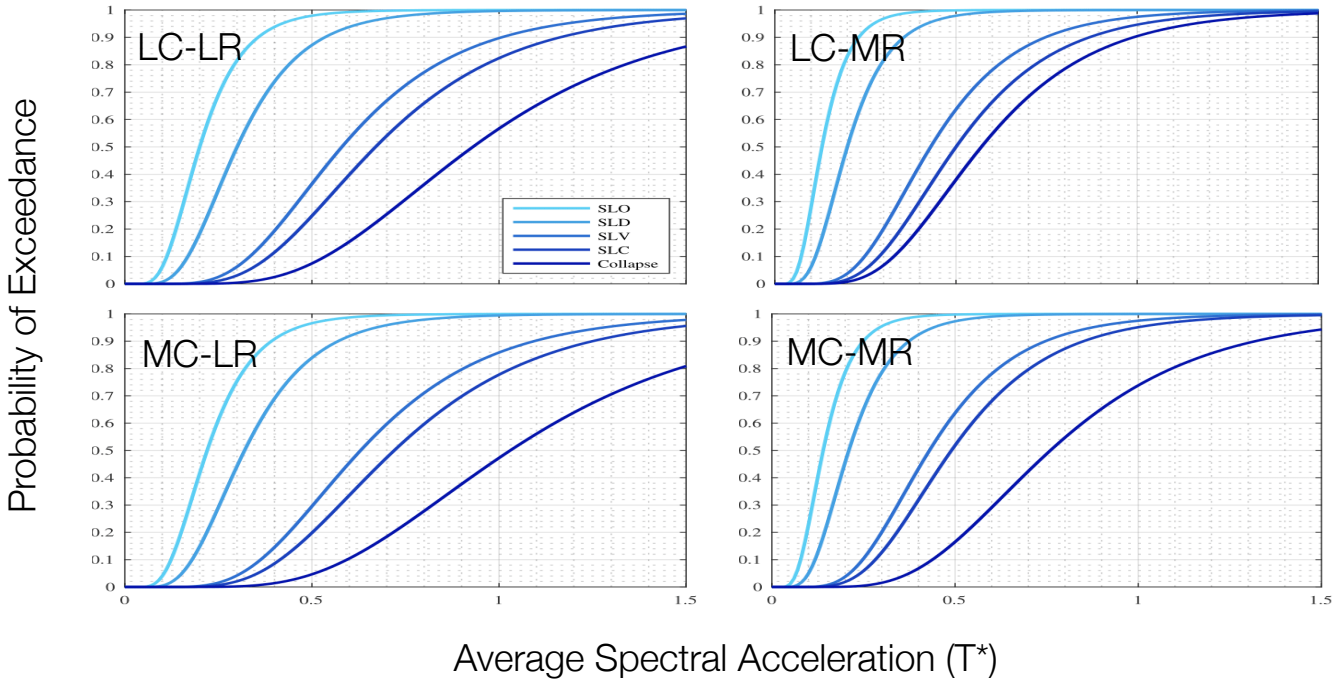
$$\underbrace{\beta_{MDL} = 0.34}$$

According to O'Reilly and Sullivan for two-to-six storey infilled RC buildings

Analytical Fragility Functions

- Analytical FFs can be derived following the assumption of lognormality which implies that the IM values of ground motions causing damage state exceedances are lognormally distributed, which is a common assumption that has been confirmed in various studies

$$P[x > DS_i | IM = im] = \Phi\left(\frac{\ln\left(im/\tilde{\eta}_{tax,IM|DSi}\right)}{\beta_{lnY_{tax,total}}}\right)$$





Empirical Fragility Functions

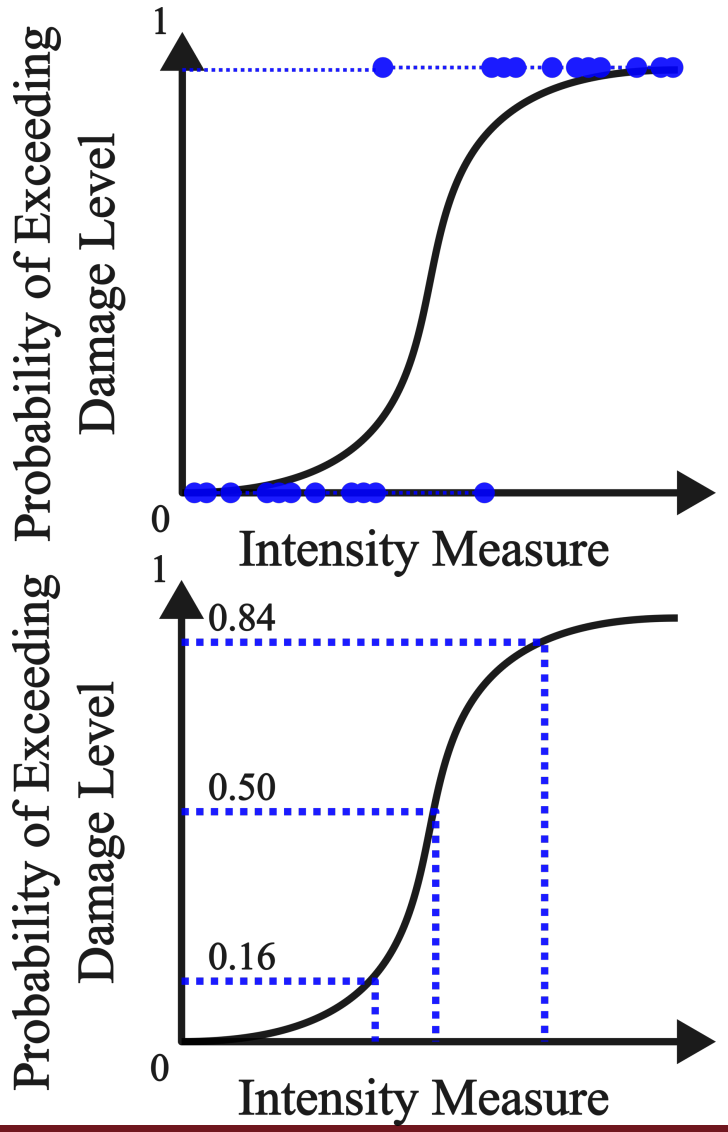
Derivation of state-of-the-art empirical fragility functions using average spectral acceleration-based ground-motion fields

General Notions

- Empirical FFs are models derived from pairs of observed damage and intensity data for buildings and infrastructure

- X-axis: Intensity measure values at points of interest are obtained either through: (1) field surveys or measurements or (2) numerical simulation using GMMs

- Y-axis: Damage data are collected for a group of surveyed and spatially-distributed exposed assets



Case Study Events

- Umbria-Marche 1997 (11:40 am on September 26th)
- Magnitude 6.2
- 11 fatalities, 100s injuries and at least 80000 displaced;





Images courtesy of: britannica.com

Case Study Events

- L'Aquila 2009 (1:32 am on April 6th)
- Magnitude 6.3
- 308 fatalities, 1500 injured and at least 66000 displaced;
- 16 billion USD in economic losses;

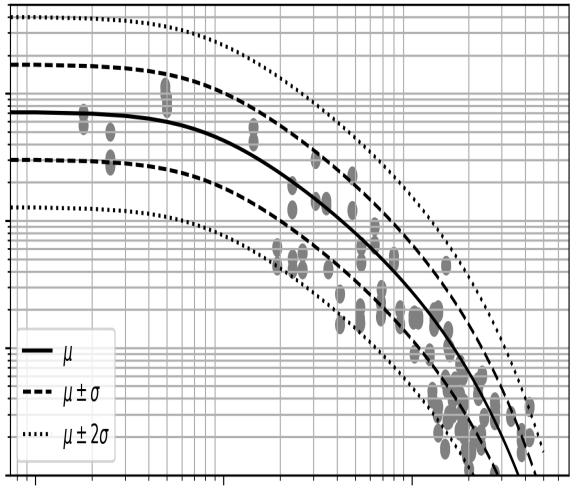




Images courtesy of: britannica.com

Mapping Intensities

- GMFs are derived using GMMs
- GMMs provide a mean of predicting the level of ground shaking and its associated uncertainty at any given site or location
- GMMs are efficiently used to estimate ground motions for use in both deterministic and probabilistic seismic hazard analyses.
- GMFs have a broad range of application:
  - Provides emphasis on the allocation of resources to speed up the recovery process
  - Overlaying GMFs with inventories of critical facilities and infrastructure provides an important means of response prioritisation
- Limitation: Their availability for conventional IMs



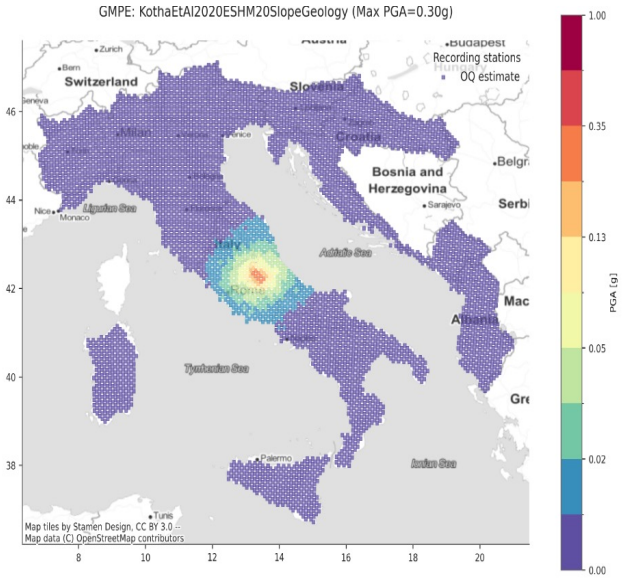


Image Reference: GEM Earthquake Scenario Database
GEM Foundation (2023), GEM Earthquake Scenario Database, GitHub. https://github.com/gem/earthquake-scenarios/
DOI: 10.5281/zenodo.8425465

Mapping Intensities

- For this application, average spectral acceleration-based GMFs are necessary
- Two approaches exist for the estimation of empirical average spectral acceleration values:
  - Direct approach: prediction via the derivation of a GMM from a strong motion dataset (i.e., compiling and processing strong motion records, establishing record selection criteria, selecting a robust GMM functional form, mixed-effects regression, model refinement through residual analysis)
  - Indirect approach: makes use of peer-reviewed GMMs for spectral acceleration to predict a distribution of average spectral acceleration

Mapping Intensities

- Two approaches exist for the estimation of empirical average spectral acceleration values:
  - Direct approach: prediction via the derivation of a GMM from a strong motion dataset (i.e., compiling and processing strong motion records, establishing record selection criteria, selecting a robust GMM functional form, mixed-effects regression, model refinement through residual analysis)
  - Indirect approach: makes use of peer-reviewed GMMs for spectral acceleration to predict a distribution of average spectral acceleration

$$\underbrace{\mu_{lnSa_{avg}}}_{\text{Mean of } \ln(Sa_{avg}(T^*))} = \frac{1}{n}\sum_{i=1}^{n} \underbrace{\mu_{\mathrm{lnSa(T}_i)}}_{\text{Mean of } \ln(Sa(T^*))}$$

$$\underbrace{\sigma^2_{lnSa_{avg}}}_{\text{Square of the standard deviation}} \overbrace{= varlnSa_{avg}}^{\text{Variance}} = \left(\frac{1}{n}\right)^2 \sum_{i=1}^{n}\sum_{j=1}^{n} \underbrace{\rho_{\mathrm{lnSa(T}_i),\mathrm{lnSa(T}_j)}}_{\text{Correlation between spectral intensities}} \overbrace{\sigma_{\mathrm{lnSa(T}_i)}\,\sigma_{\mathrm{lnSa(T}_j)}}^{\text{Logarithmic standard deviations}}$$

Mapping Intensities

- For this regional application, the GMM proposed by Bindi *et al.* was used to evaluate the spectral intensities at distinct periods ranging from 0.04-2.0*s*
- The GMM allows for the estimation of ground-shaking intensities (PGA, Sa(T)) corresponding to magnitude range of 4-6.9 and considering distances up to 200 km.

Distance function

Soil amplification and style of faulting functions

$$\underbrace{\log_{10} SA(T^*)}_{\text{Logarithm of the mean spectral acceleration}} = e_1 + \overbrace{F_D(R,M)}^{\text{Distance function}} + \underbrace{F_M(M)}_{\text{Magnitude function}} + \overbrace{F_s + F_{sof}}^{\text{Soil amplification and style of faulting functions}}$$

Ground-Motion Model Conditioning

Ground-Motion Model Conditioning: Engler *et al.* (2022)

$$\underbrace{\ln im_{i,j}}_{\text{Observation}} = \overbrace{\mu_{IM}\left(rup_i, site_j\right)}^{\text{Prediction (GMM)}} + \underbrace{\delta B_i + \delta W_{i,j}}_{\text{Between- and within-event residuals}}$$

(station registration)

$$\delta B_i = \frac{\tau^2 \sum_{j=1}^{n_i} \Delta_{i,j}}{n_i \tau^2 + \phi^2}$$

$$\ln im_{i,j} = \left(\mu_{IM}\left(rup_i, site_j\right) + \delta B_i\right) + \delta W_{i,j}$$

Ground-Motion Model Conditioning

Ground-Motion Model Conditioning: Engler *et al.* (2022)

$$\ln im_{i,j} = \mu_{IM}\left(rup_i, site_j\right) + \delta B_i + \delta W_{i,j}$$

$$\delta B_i = \frac{\tau^2 \sum_{j=1}^{n_i} \Delta_{i,j}}{n_i \tau^2 + \phi^2}$$

τ: inter-event variability;

ϕ: intra-event variability;

n: number of observations;

$\Delta_{i,j} = \delta B_i + \delta W_{i,j}$;

i, j : i-th event, j-th observation

$$\ln im_{i,j} = \left(\mu_{IM}\left(rup_i, site_j\right) + \delta B_i\right) + \delta W_{i,j}$$

Ground-Motion Model Conditioning

Ground-Motion Model Conditioning: Engler *et al.* (2022)

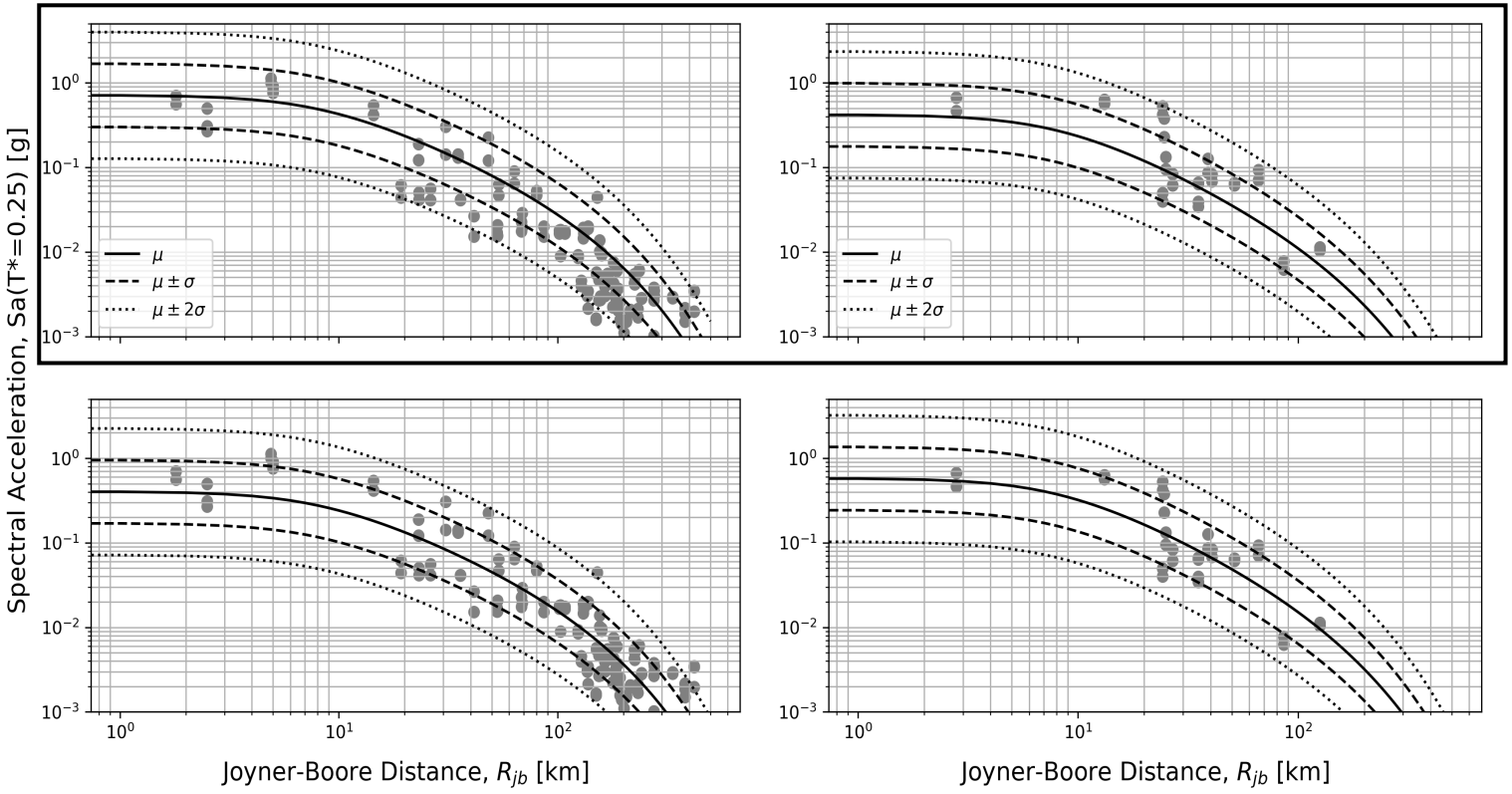
$$\ln im_{i,j} = \mu_{IM}\left(rup_i, site_j\right) + \delta B_i + \delta W_{i,j}$$

$$\delta B_i = \frac{\tau^2 \sum_{j=1}^{n_i} \Delta_{i,j}}{n_i \tau^2 + \phi^2}$$

$$\ln im_{i,j} = \underbrace{\left(\mu_{IM}\left(rup_i, site_j\right) + \delta B_i\right)}_{} + \delta W_{i,j}$$

Ground-Motion Model Conditioning

Before Conditioning

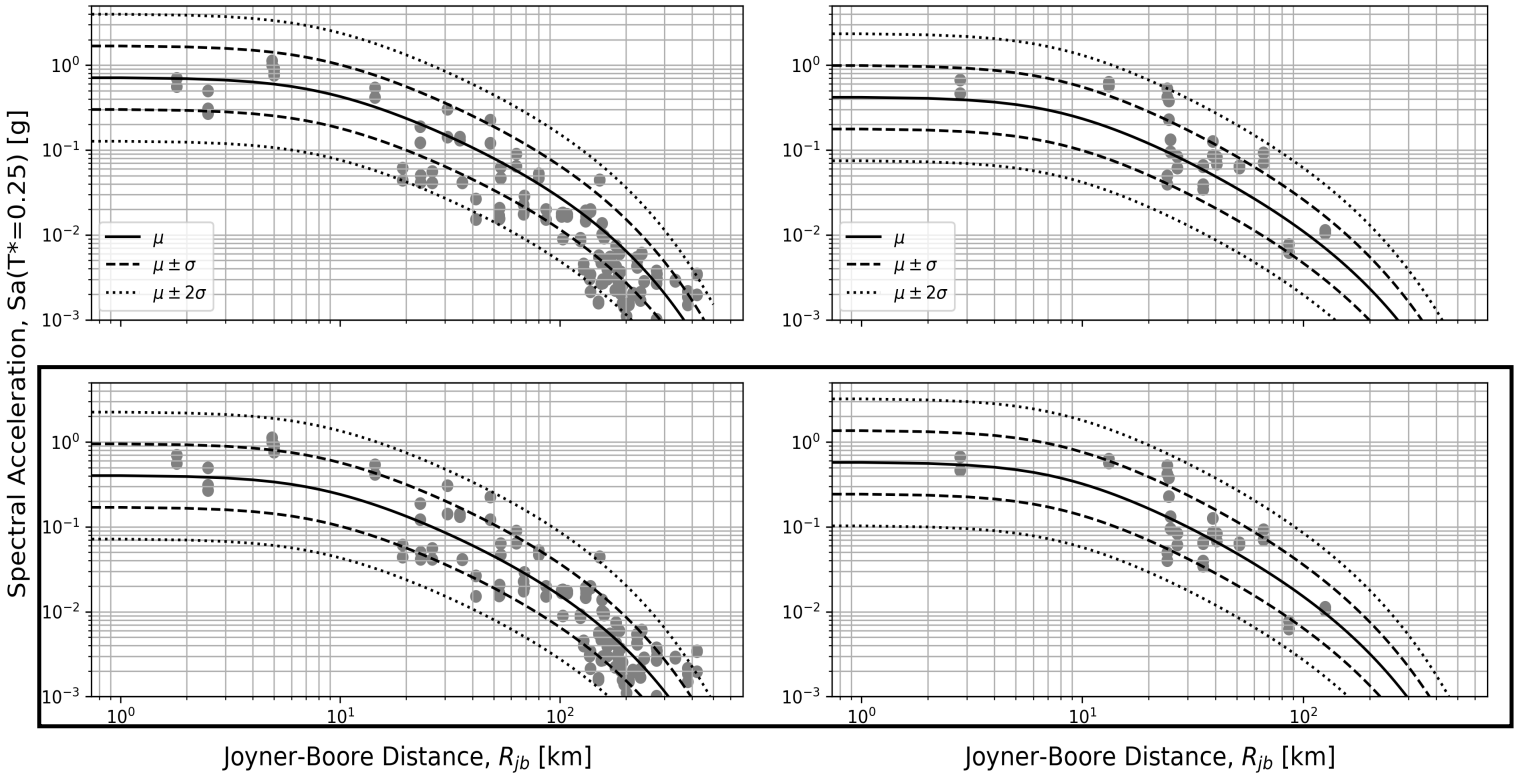


Umbria-Marche

L'Aquila

Ground-Motion Model Conditioning

After Conditioning



Umbria-Marche

L'Aquila

Spatial Correlation

- Spatial dependence among ground motions typically impacts predicted consequences to spatially distributed assets
- Spatial correlation considers spatial dependence in the joint probability distribution function of an intensity measure given a rupture scenario
- Considering spatial correlation yields the most accurate estimates
- A model which does not account for spatial correlation implies that larger-than-median motions would occur at individual locations independently.
- Spatial correlation model for the average spectral acceleration derived by Heresi and Miranda (2021) was adopted in this study

$$\boldsymbol{R} = \rho_{lnSa_{avg,i}lnSa_{avg,j}} = \frac{\frac{1}{100}\sum_{k=1}^{10}\sum_{l=1}^{10}\rho_{lnSa_{k,i},lnSa_{l,j}}.\sigma_{lnSa_{k,i}}.\sigma_{lnSa_{l,j}}}{\sigma_{lnSa_{avg,i}}.\sigma_{lnSa_{avg,j}}}$$

GMF Simulation

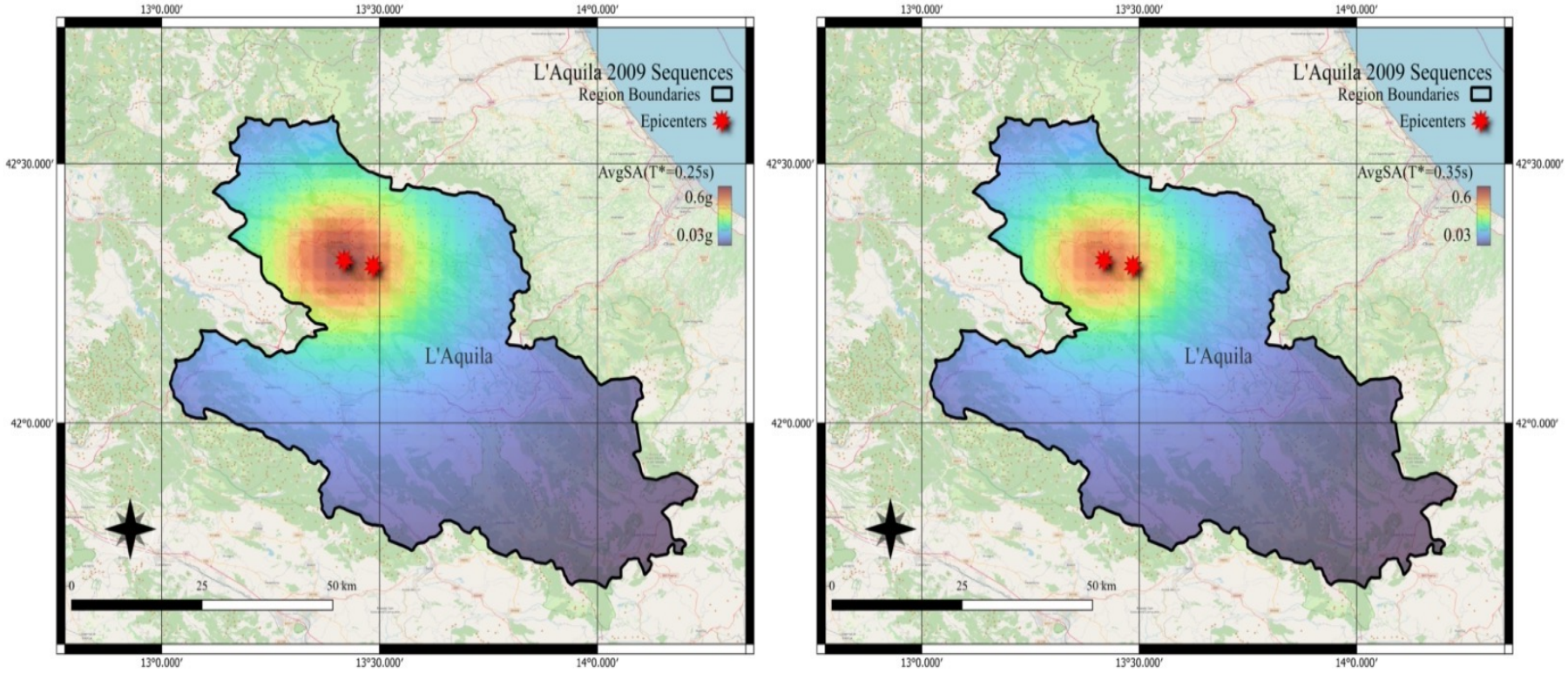
$$\ln \boldsymbol{IM} \sim \mathcal{N}(\boldsymbol{M}, \boldsymbol{\Sigma})$$

$$\boldsymbol{M} = \begin{bmatrix} \ln \mu_{IM}(rup_i, site_1) \\ \ln \mu_{IM}(rup_i, site_n) \\ \cdots \\ \ln \mu_{IM}(rup_i, site_n) \end{bmatrix}$$

$$\boldsymbol{\Sigma} = \begin{bmatrix} \sigma^2_{lnIM_{i,1}} & \cdots & \sigma_{lnIM_{i,1},lnIM_{i,n}} \\ \vdots & \ddots & \vdots \\ \sigma_{lnIM_{i,n},lnIM_{i,1}} & \cdots & \sigma^2_{lnIM_{i,n}} \end{bmatrix} = \tau^2 \boldsymbol{I} + \phi^2 \boldsymbol{R}$$

GMF Simulation

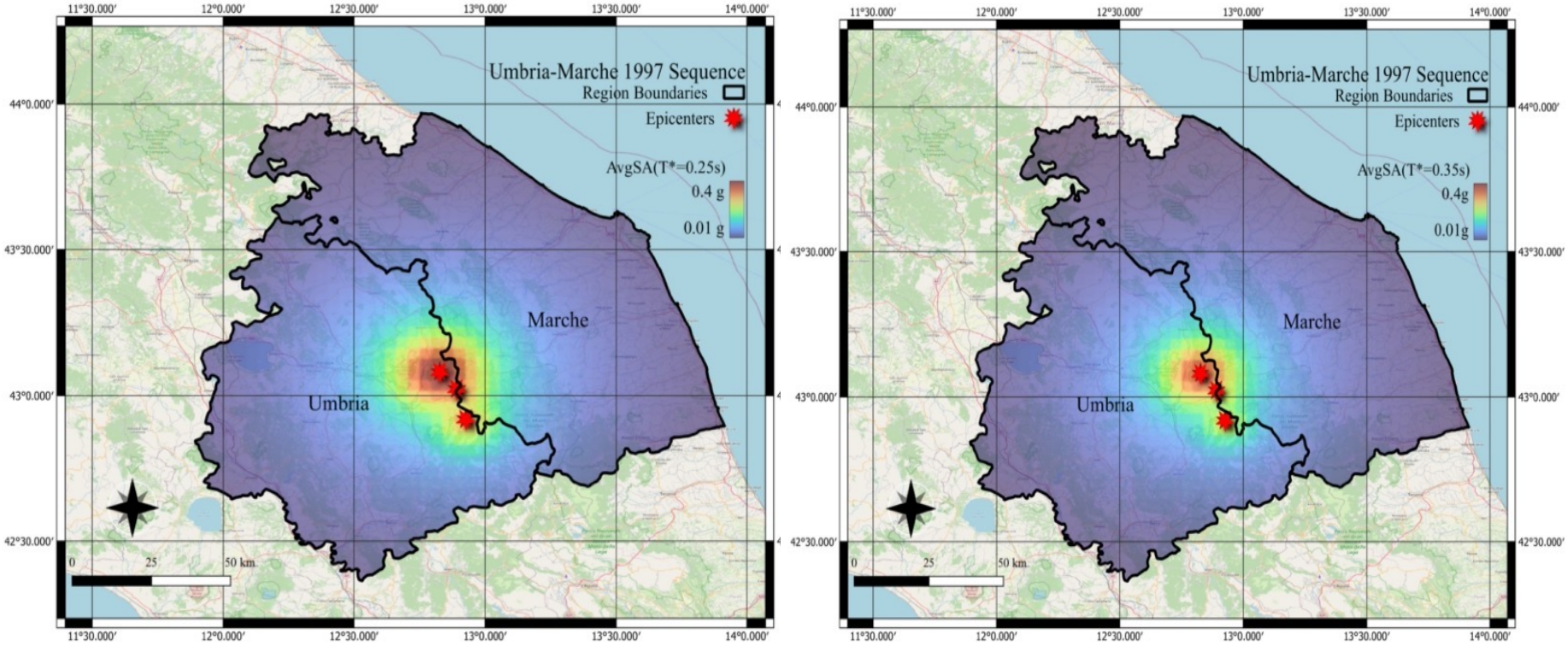
- GMFs for L'Aquila 2009 event



Average spectral acceleration GMFs for T*=0.25s (left) and 0.50s (right)

GMF Simulation

- GMFs for Umbria-Marche 1997 event

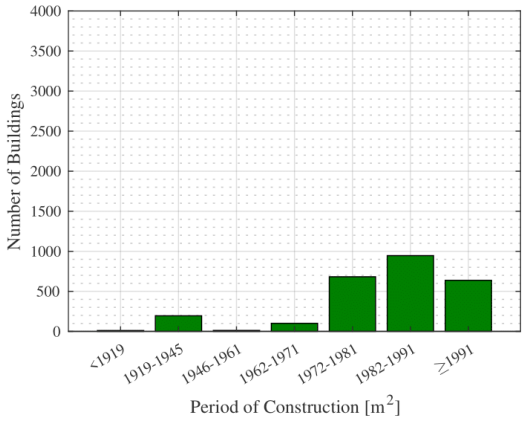


Average spectral acceleration GMFs for T*=0.25s (left) and 0.50s (right)

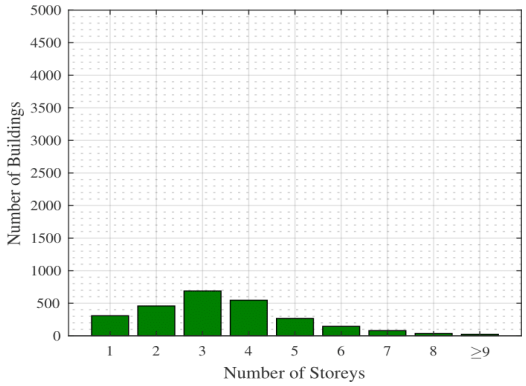
Damage Characterisation

- Da.D.O. (Database of Observed Damage) is an IT platform and database to collect, data on the structural characteristics and the observed damage of buildings inspected after the most relevant seismic events occurred in Italy from the Friuli 1976 earthquake onwards
- 2164 RC buildings were surveyed following the Umbria-Marche 1997 event

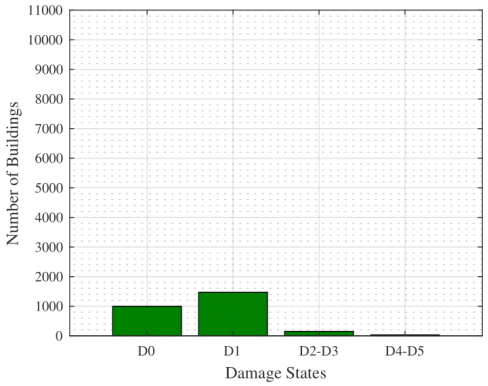
Period of Construction



Number of Storeys



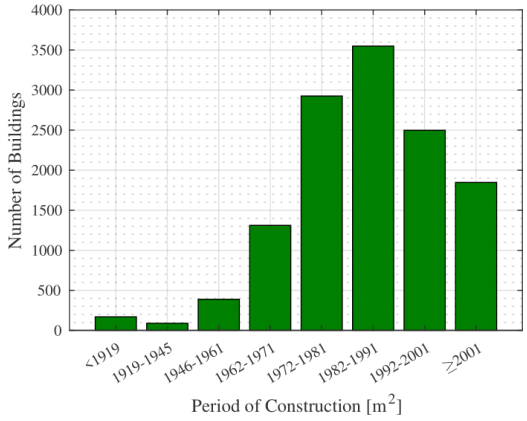
Damage States



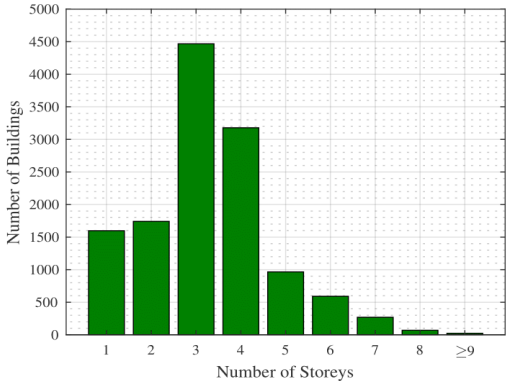
Damage Characterisation

- Da.D.O. (Database of Observed Damage) is an IT platform and database to collect, data on the structural characteristics and the observed damage of buildings inspected after the most relevant seismic events occurred in Italy from the Friuli 1976 earthquake onwards
- 2164 RC buildings were surveyed following the Umbria-Marche 1997 event
- 8502 RC buildings were surveyed following the L'Aquila 2009 event

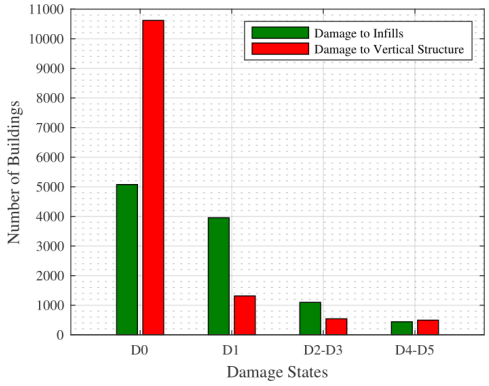
Period of Construction



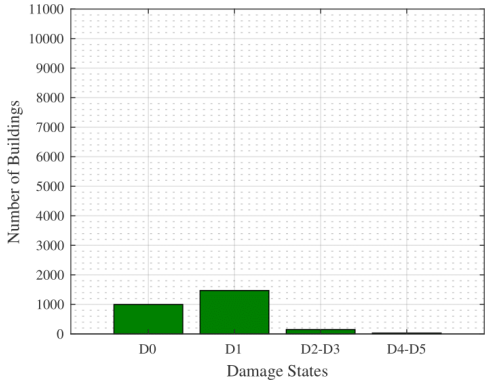
Number of Storeys



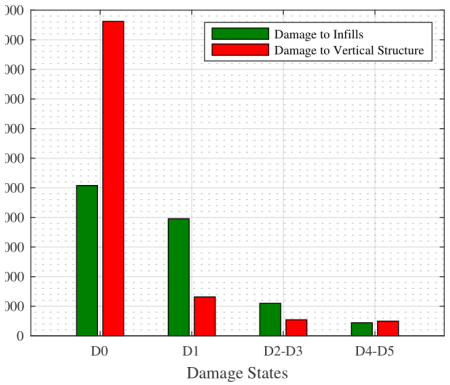
Damage States



Damage Characterisation



Umbria-Marche



L'Aquila

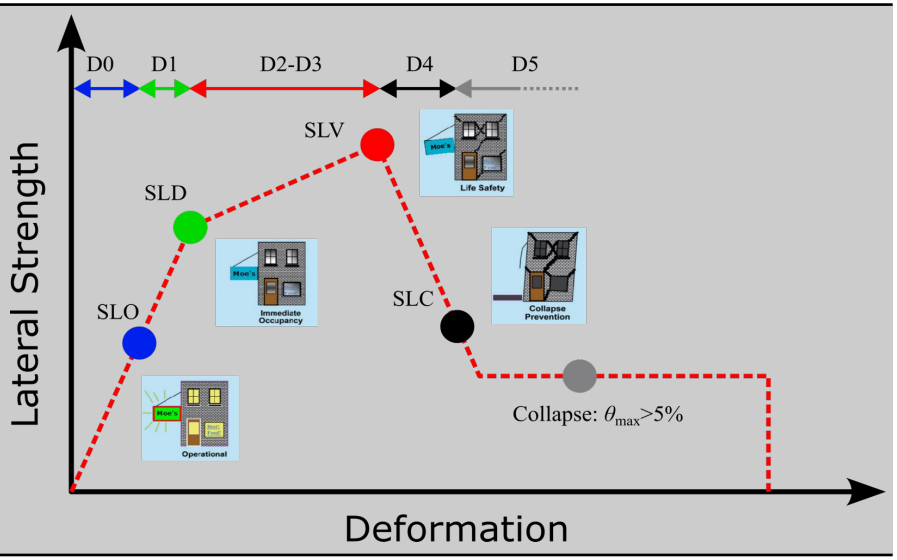
After 1997

Before 1997

AeDES Damage Scales	EMS-98 Damage Scales		Structural Damage	Non-Structural Damage
D0	Grade 0 (DS0)	No damage	No	No
D1	Grade 1 (DS1)	Negligible to slight damage	No	Slight
D2-D3	Grade 2 (DS2)	Moderate damage	Slight	Moderate
	Grade 3 (DS3)	Substantial to heavy damage	Moderate	Heavy
D4-D5	Grade 4 (DS4)	Very heavy damage	Heavy	Very Heavy
	Grade 5 (DS5)	Destruction	Very Heavy	Very Heavy

Damage Characterisation

- Damage state harmonization is necessary to establish a link between analytical and empirical FFs
- The following assumption on DSs equivalency was proposed

AeDES Damage State	Hybrid Limit State	Primary Objective	Graphical Illustration
D0	SLO	Functionality and usability of the building	
D1	SLD	Safety and immediate occupancy;	
D2-D3	SLV	Protection of occupants' lives and ensurance of safe evacuation	
D4	SLC	Structural collapse prevention;	
D5	Collapse	Structural collapse	

Fitting Empirical Fragility Functions

- Given the availability of building-by-building data, the Bernoulli distribution is selected for characterizing the random component of the statistical model

$$Y_{ij}|IM = im_j \sim \binom{n_j}{y_{ij}} p_{ij}{}^{y_{ij}} [1 - p_{ij}]^{(n_j - y_{ij})} = \begin{cases} 1 \\ 0 \end{cases}$$

- $Y_{ij}|IM$ indicates whether asset *i* is in damage state *j*
- For a certain damage level, all exposed assets with an observed damage level D<Di will have a probability equal to zero
- For a certain damage level, all exposed assets with an observed damage level D>Di will have an assigned probability equal to unity
- The adoption of the Bernoulli distribution, which is a special case of the binomial distribution, allows for avoiding aggregation of damage data, which may introduce uncertainty in the resulting fragility estimates

Fitting Empirical Fragility Functions

- the derivation of FFs requires an appropriate statistical model and fitting technique to approximate observational data as a function of the ground motion severity.
- The cumulative lognormal distribution is adopted for describing the probability of reaching or exceeding a preselected damage level, as a function of the seismic intensity measure:

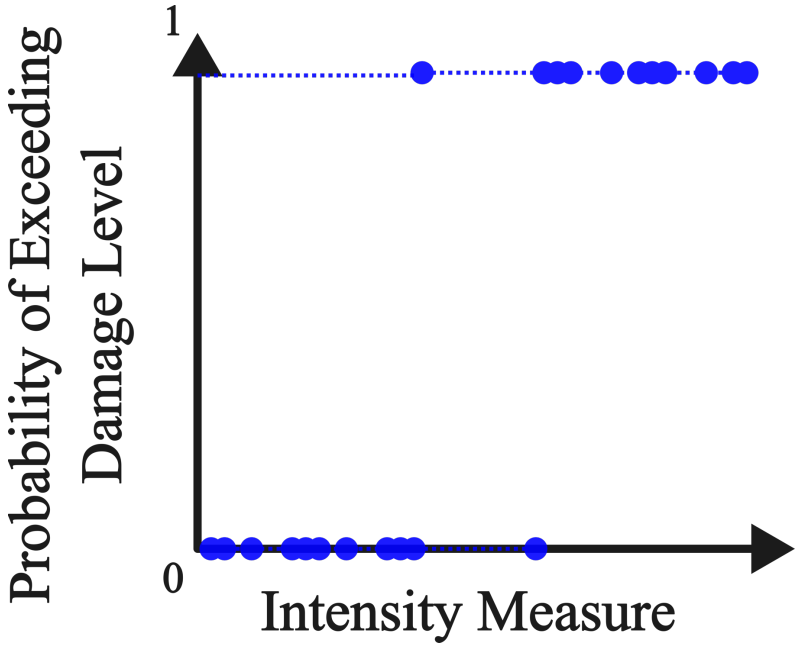
$$P\left(DS \geq ds_i \middle| IM = im_j\right) = \Phi\left[\frac{\log(im_j/\theta_{ds_i})}{\beta}\right]$$

- Fragility functions are simultaneoulsy fitted via the maximum likelihood estimate approach
- For each taxonomy, optimal parameters of the fragility model result from maximising the logarithm of the likelihood function:

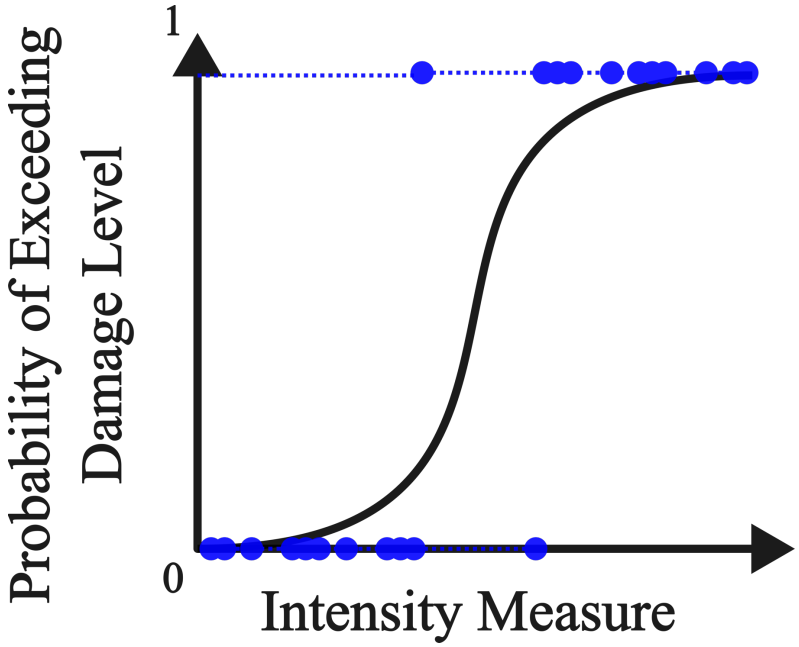
$$\theta_{ds_i}, \beta = argmax\left[\log\left(\prod_{i=1}^{nDS}\prod_{j=1}^{N}\frac{n_j!}{y_{ij}!\left(n_j - y_{ij}\right)}{p_{ij}}^{y_{ij}}(1-p_{ij})^{(n_j - y_{ij})}\right)\right]$$

Fitting Empirical Fragility Functions

Applying Bernoulli distribution to random component (Slide 56)

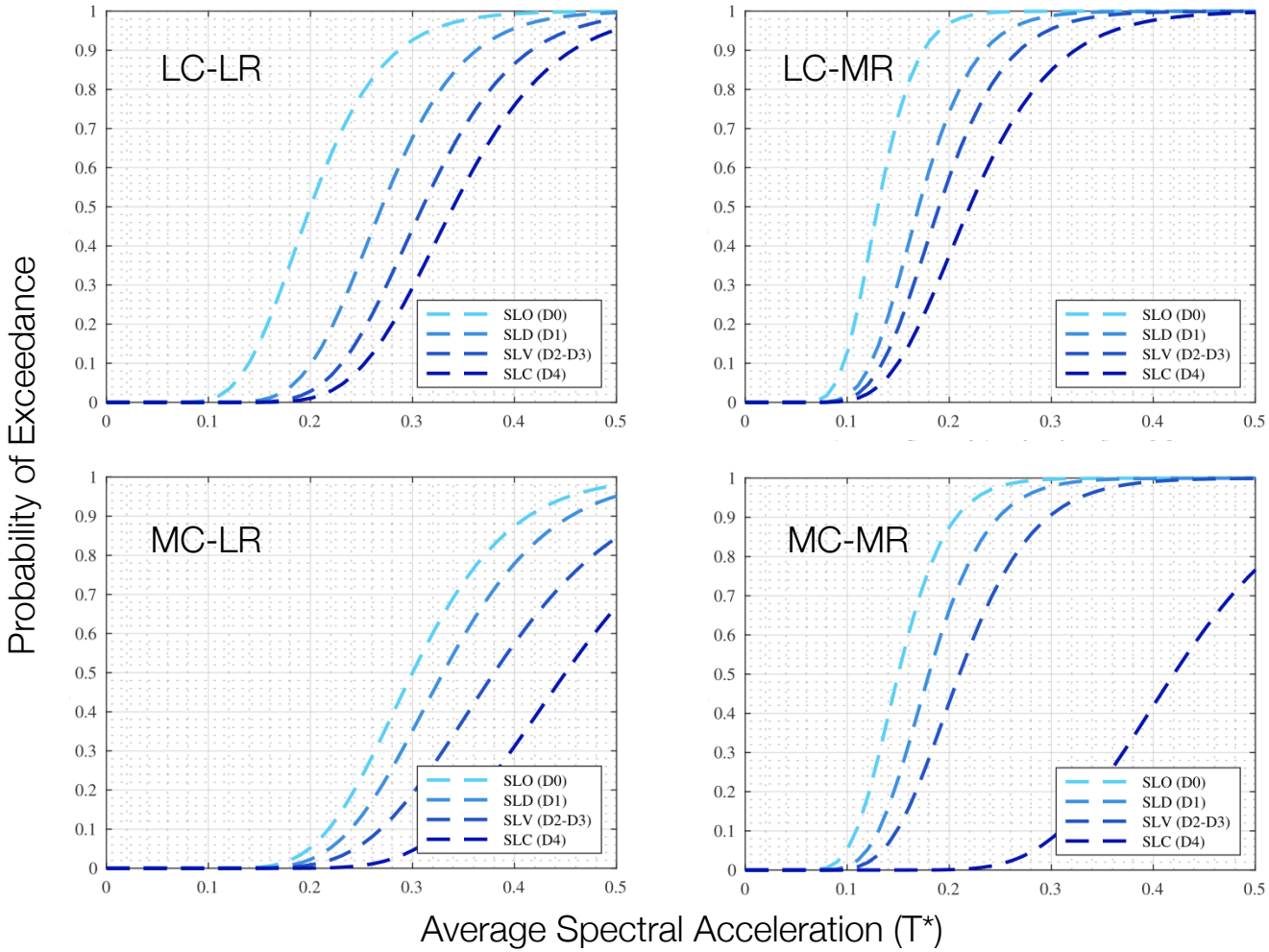


Fitting lognormal CDF using maximum likelihood estimation(Slide 57)



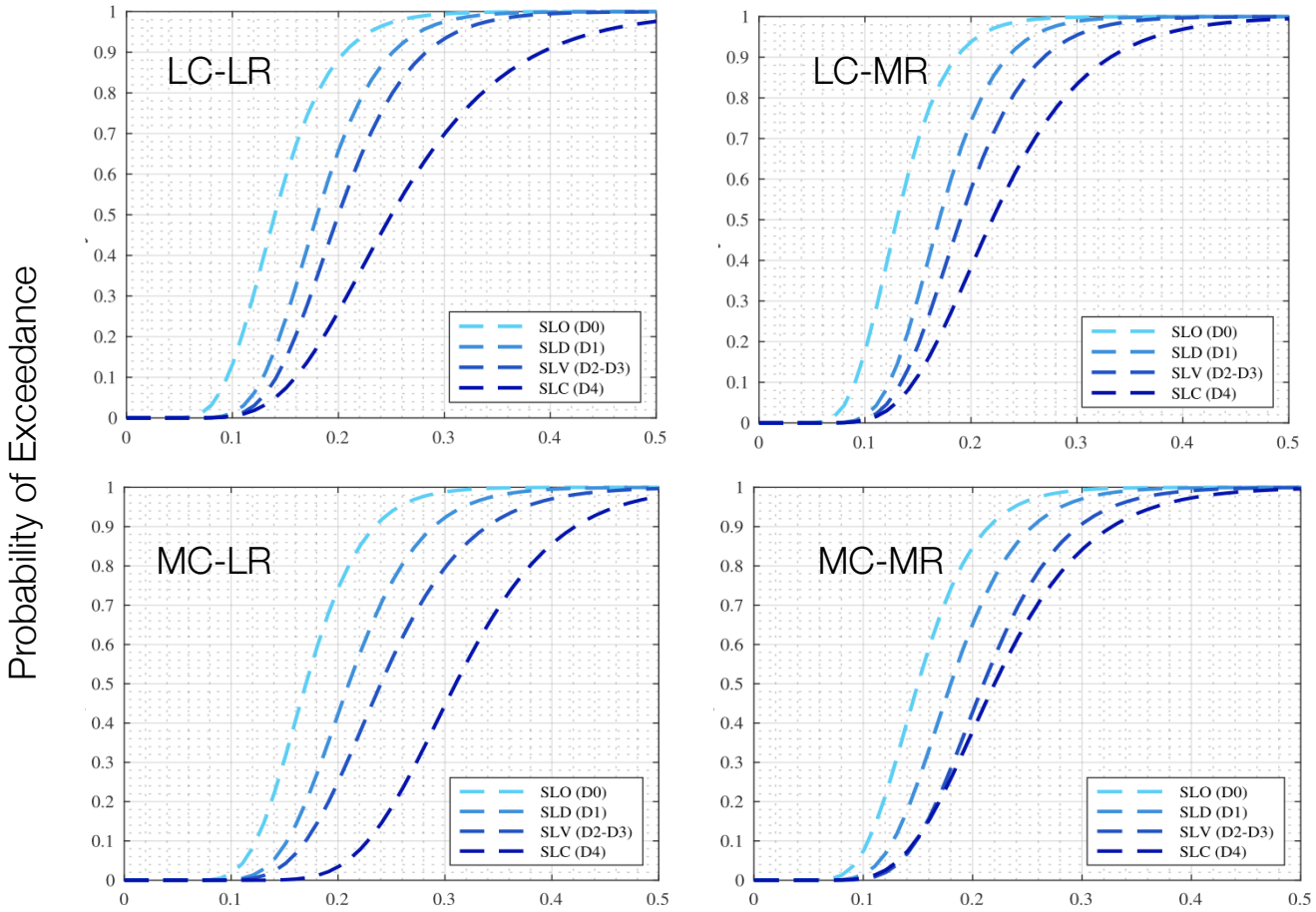
Empirical Fragility Functions

- Empirical Fragility Functions: Umbria-Marche 1997



Empirical Fragility Functions

- Empirical Fragility Functions: L'Aquila 2009

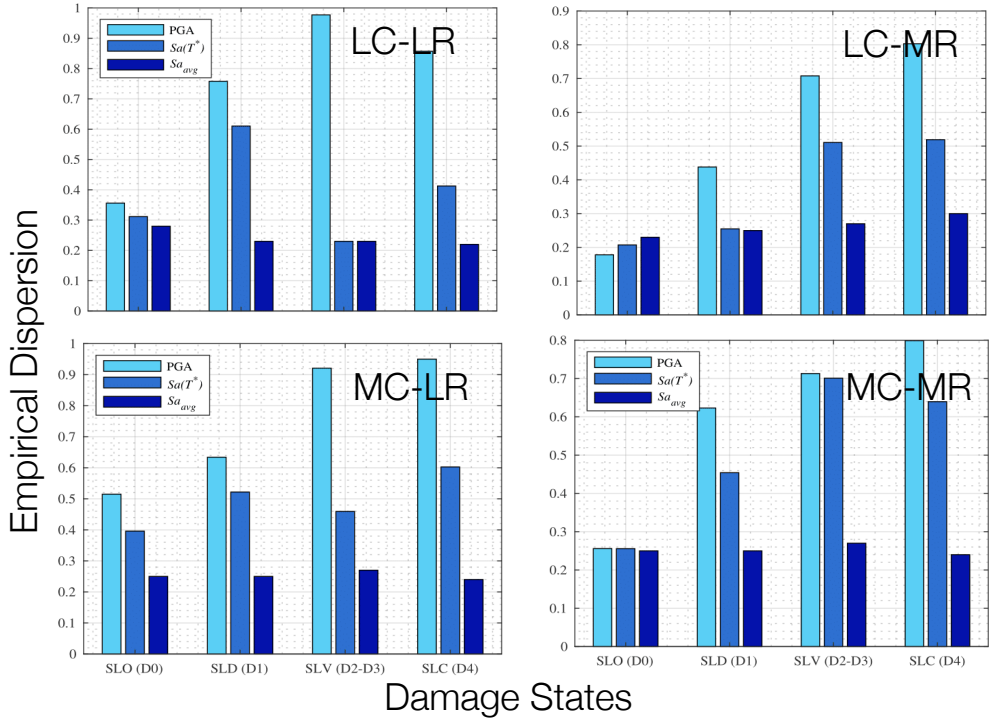




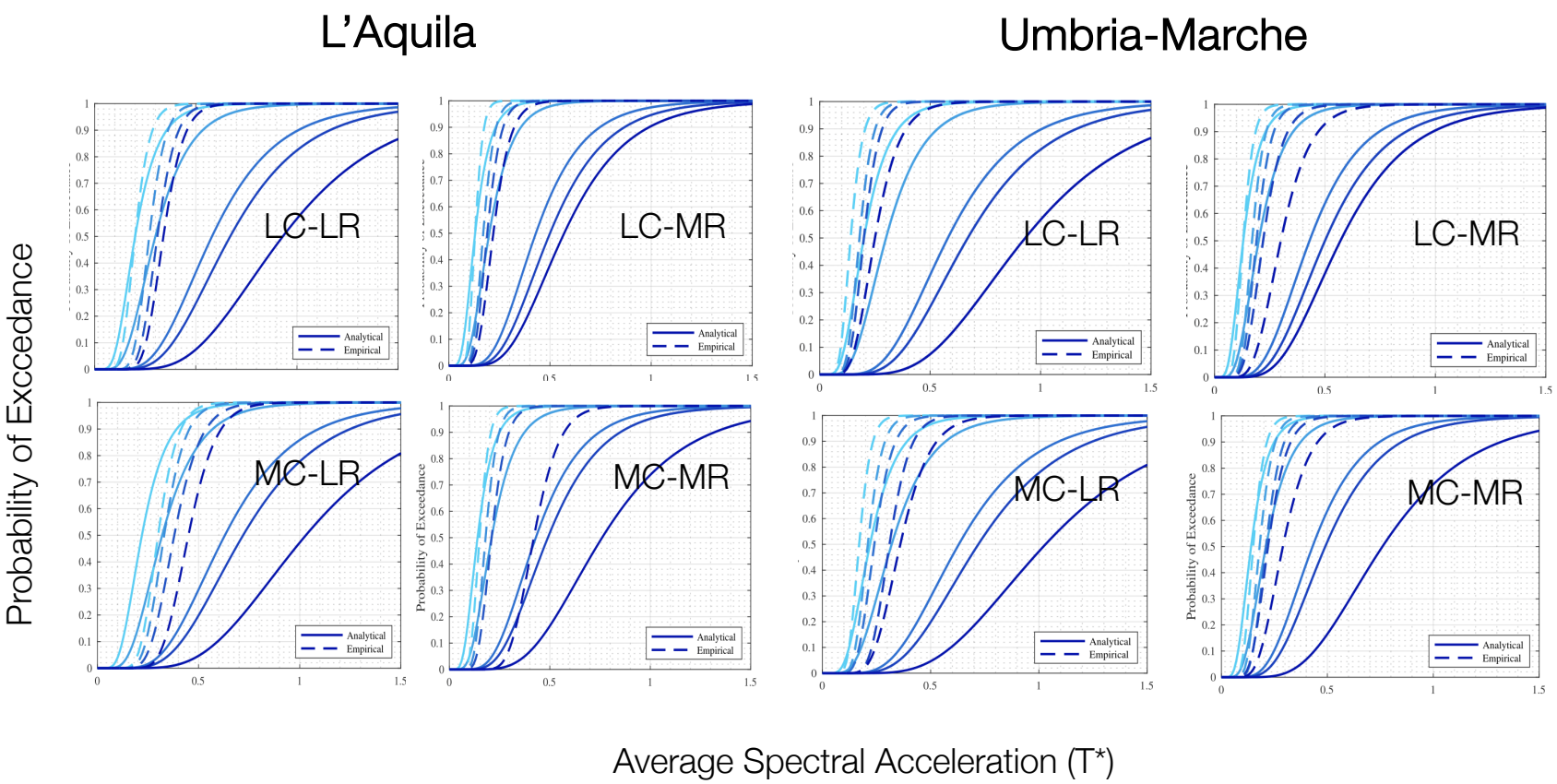
Verification & Conclusions

Verification & Discussion

- The reduction of uncertainty in FFs is crucial for improving the accuracy and reliability of seismic risk applications.
- Reducing uncertainty was demonstrated to be achieved using more efficient IMs.
- Results demonstrate that choosing appropriate IMs is beneficial as the choice directly influences the robustness of fragility functions, and via the concept of uncertainty propagation in PBEE, the estimation of decision variable



Verification & Discussion



Verification & Discussion

- Damage accumulation in buildings following earthquake sequences
- The assumptions associated with the anchoring period for the empirical fragility functions
- The uncertainty in the damage states definition between empirical and analytical fragility functions
- The bias in data collection due to the differences in damage state perception between one expert and another

Conclusions

- Fragility functions (FFs) are used worldwide for single-building and regional seismic risk and loss applications
- Previous studies have opted to use conventional IMs such as PGA and spectral acceleration for the derivation of analytical and empirical fragility functions
- Novel FFs for the infilled RC building classes were derived analytically the average spectral acceleration was considered as IM
- The analytical FFs consider all sources of uncertainty (i.e., record-to-record variability, building-to-building variability, modelling uncertainty)
- Empirical FFs were derived using Saavg-based GMFs conditioned on instrumental/station data to account for the “ground truth” and damage observations
- The average spectral acceleration offers a more reliable characterization of structural vulnerability highlighted by the low associated variability compared to more conventional IMs for the empirical case
- Analytical FFs consistently overestimated the seismic intensities across the range of structural response (i.e. across damage states)

Future Work

- Sensitivity analyses on the period range associated with the average spectral acceleration
- Simulation/Testing of GMFs using more GMMs
- Running NLTHA accounting for damage accumulation (mainshock-aftershock sequences)
- Characterisation of a more adequate relationship between code-based limit states and empirical damage states

References

- Eads L, Miranda E, Lignos DG. Average spectral acceleration as an intensity measure for collapse risk assessment. *Earthquake Engineering and Structural Dynamics* 2015; 44(12): 2057–2073. DOI: 10.1002/eqe.2575.

- Kurukulasuriya M, Milanesi R, Bolognini D, Lanese I, Grottoli L, Magenes G, *et al.* Shaking table experimental campaign on pre-code masonry infills subjected to in-plane and out-of- plane loading. *SPONSE*, Stanford, California: 2022.

- Kurukulasuriya M, Milanesi R, Magenes G, Bolognini D, Grottoli L, Dacarro F, Morandi P, Investigation of seismic behaviour of existing masonry infills through combined cyclic in-plane and dynamic out-of-plane tests, 9th *COMPDYN* , Athens, Greece: 2023.

- Danciu L., Nandan S., Reyes C., Basili R., Weatherill G., Beauval C., Rovida A., Vilanova S., Sesetyan K., Bard P-Y., Cotton F., Wiemer S., Giardini D. (2021) - The 2020 update of the European Seismic Hazard Model: Model Overview. EFEHR Technical Report 001, v1.0.0, https://doi.org/10.12686/a15

- Mori F, Mendicelli A, Moscatelli M, Romagnoli G, Peronace E, Naso G. A new Vs30 map for Italy based on the seismic microzonation dataset. *Engineering Geology* 2020; **275**: 105745. DOI: 10.1016/j.enggeo.2020.105745.

References

- Jalayer F, Cornell CA. Alternative non-linear demand estimation methods for probability-based seismic assessments. *Earthquake Engineering and Structural Dynamics* 2009; **38**(8): 951–972. DOI: 10.1002/eqe.876.

- Kohrangi M, Kotha SR, Bazzurro P. Ground-motion models for average spectral acceleration in a period range: Direct and indirect methods. *Bulletin of Earthquake Engineering* 2018; **16**(1): 45–65. DOI: 10.1007/s10518-017-0216-5.

- Wald DJ, Quitoriano V, Heaton TH, Kanamori H, Scrivner CW, Worden CB. TriNet "ShakeMaps": Rapid Generation of Peak Ground Motion and Intensity Maps for Earthquakes in Southern California. *Earthquake Spectra* **15**(3): 537–555.

- Worden CB, Thompson EM, Hearne M, Wald DJ. *ShakeMap manual: technical manual, user's guide, and software guide*. 2020. DOI: https://doi.org/10.5066/F7D21VPQ.

- Heresi P, Miranda E. Intensity Measures for Regional Seismic Risk Assessment of Low-Rise Wood-Frame Residential Construction. *Journal of Structural Engineering* 2021; **147**(1). DOI: 10.1061/(ASCE)ST.1943-541X.0002859.

References

- Lallemant D, Kiremidjian A, Burton H. Statistical procedures for developing earthquake damage fragility curves. *Earthquake Engineering & Structural Dynamics* 2015; **44**(9): 1373–1389. DOI: 10.1002/eqe.2522.

- 114. Nguyen M, Lallemant D. Order Matters: The Benefits of Ordinal Fragility Curves for Damage and Loss Estimation. *Risk Analysis* 2022; **42**(5): 1136–1148. DOI: 10.1111/risa.13815.

- Rosti A, Smerzini C, Paolucci R, Penna A, Rota M. Validation of physics-based ground shaking scenarios for empirical fragility studies: the case of the 2009 L'Aquila earthquake. *Bulletin of Earthquake Engineering* 2023; **21**(1): 95–123. DOI: 10.1007/s10518-022-01554-1.

- O'Reilly GJ, Sullivan TJ. Quantification of modelling uncertainty in existing Italian RC frames. *Earthquake Engineering & Structural Dynamics* 2018; **47**(4): 1054–1074. DOI: 10.1002/eqe.3005.

- Engler, Davis T., C. Bruce Worden, Eric M. Thompson, Kishor S. Jaiswal (2022). Partitioning Ground Motion Uncertainty When Conditioned on Station Data. *Bull. Seism. Soc. Am.* 2022; doi: https://doi.org/10.1785/0120210177

Useful Links

- Link to database of infilled RC building models: https://github.com/gerardjoreilly/Infilled-RC-Building-Database
- Link to EzGM toolbox for ground-motion selection: https://github.com/volkanozsarac/EzGM
- Link to OpenQuake Engine: https://github.com/gem/oq-engine
- Link to DaDO database of surveyed buildings: https://egeos.eucentre.it/danno_osservato/web/danno_osservato?lang=EN


THANK YOU! Questions?